Forecasting the Reliability of Components Subjected to Harmonics Generated by Power Electronic Converters

Giovanni Mazzanti [1,*] **, Bassel Diban** [1] **, Elio Chiodo** [2] **, Pasquale De Falco** [3] **and Luigi Pio Di Noia** [4]

[1] Department of Electrical, Electronic and Information Engineering "Guglielmo Marconi", University of Bologna, 40136 Bologna, Italy; bassel.diban2@unibo.it

[2] Department of Industrial Engineering, U University of Naples Federico II, 80125 Naples, Italy; chiodo@unina.it

[3] Department of Engineering, University of Napoli Parthenope, 80143 Naples, Italy; pasquale.defalco@uniparthenope.it

[4] Department of Electrical Engineering and Information Technology, University of Naples Federico II, 80125 Naples, Italy; luigipio.dinoia@unina.it

[*] Correspondence: giovanni.mazzanti@unibo.it

check for updates

Abstract: This paper aims at refining an experimentally based reliability model for the insulation of power components subjected to the randomly varying harmonics generated by power electronic converters. Compared to previous papers of the same authors and to the existing literature, here the model is re-formulated from the theoretical viewpoint focusing on the foremost role played by low percentiles of time to failure—in particular by the 1st percentile—selected as the rated life in the framework of modern probabilistic design of components. This is not only more correct from the viewpoint of component design, but also on the safe side as for the reliability of devices. Moreover, the application of the model is broadened to treat the whole sequence of odd voltage harmonics from the 5th to the 25th, i.e., those taken as the most significant in power systems according to international standards. The limits to voltage distortion set in Standard EN50160 are the reference for establishing parametrically a series of typical distorted voltage waveshape analyzed in the applicative part, which account for the possible phase-shift angles between voltage harmonics. The effect of current harmonics is also considered, from both the theoretical and applicative viewpoint. As a last, but not least novelty, the reliability model is used here for life and reliability estimates not only of Medium Voltage (MV)/Low Voltage (LV) capacitors and cables—already studied in the previous stages of this investigation—but also of induction motors and transformers in the presence of harmonics from power converters.

Keywords: current harmonics; voltage harmonics; power electronic converters; reliability; cables; capacitors

1. Introduction

The worldwide diffusion of electric transportation systems and of smart grid technologies call for better performance of power electronic converters and components. However, in turn power electronic devices are well known to act as distorting loads, which inject voltage and current harmonics into the alternating current (AC) grid. These harmonics may hamper the reliability of power components—such as cables, capacitors, transformers, electrical motors—connected to the grid, because of the potential increase of thermal and electrical stress associated with current and

voltage harmonics. Such a situation raises the reliability challenges to power components in electric transportation systems and smart grid installations. For this reason, in the last three decades some international standards have set distortion limits. IEEE 519 in 1993 [1] established limits to voltage and current harmonics, but later on IEC 61000-2-2 [2], IEC 61000-2-4 [3], EN 50160 [4] set limits to voltage distortion only, by fixing the maximum values of low-order voltage harmonics in LV/MV grids in unperturbed conditions.

Forecasting the reliability of the components in the presence of current and voltage harmonics is not an easy task. Traditional approaches rely on accelerated life testing (ALT) and on historical failure databases, but the fast technological development-leading to highly reliable devices-and the difficulty of performing sound testing campaigns under harmonic distortion make these data hardly available. The estimation of reliability in distorted conditions is made more difficult by the random nature of harmonic distortion brought about by power electronic devices. This requires proper statistical models and methods capable of correlating the electric and thermal stress, associated with voltage and current harmonics, to life and the reliability of components.

To overcome all these difficulties, a probabilistic electro-thermal life model—that can also be referred to as "electro-thermal reliability model" [5]—has been developed and proved to be capable of forecasting the life and reliability of components subjected to randomly time-varying harmonics generated by power electronic converters [6–9]. This model is based on a broad and innovative experimental campaign of testing insulating specimens (flat samples, mini-cables, twisted pairs) for power components (cables, capacitors, transformers, rotating machines) subjected to a big deal of combinations of voltage harmonics, as shown in [10–13]. Other tests of this kind are described e.g., in [14–18], but with particular emphasis on water tree growth in cross-linked polyethylene (XLPE) insulation for power cables in a wet environment. However, results of aging tests of insulation under distorted voltage are rare in the literature, due to the experimental difficulties in arranging test set-ups for aging of insulation in the presence of distorted voltage. For this reason, attention in the literature of reliability models under harmonic distortion is mainly concentrated on the thermal effect of current harmonics [19–23] although applications relevant to the electrical aging can also be found e.g., in [24–30].

Following the streamline of this investigation over the years, in the very first application of this electro-thermal reliability model for insulation under harmonic distortion the level of distortion was either set parametrically [6] or derived experimentally for a particular case [7]. Then, the model was used to estimate the reliability of MV/LV components affected by voltage harmonics matching exactly the limits established in [4] (which are numerically the same as those in [2,3]); the study was broadened from the 11th, 13th voltage harmonics treated in [8], to the combination of the 5th, 7th, 11th, 13th treated in [9], showing that—notwithstanding the compliance with [4]—the reliability of components decreased significantly with respect to rated sinusoidal conditions.

Here, as the ultimate stage of the investigation specifically conceived for this Special Issue, the reliability model is refined and better formulated from the theoretical viewpoint. Furthermore, its application is significantly broadened in this paper, since here many new case studies are examined and two more power system components (induction motors and transformers) are treated in addition to those (cables and capacitors) already studied in the previous stages of this investigation. The main novelties in this paper compared to previous papers devoted to the same topic [8,9] are as follows.

From the theoretical viewpoint, in our previous papers and in the existing literature the theory of life and reliability estimation of the insulation of components in distorted conditions relied on the 63.2th percentile of failure time and on the mean time to failure (MTTF). Here, in the theoretical treatment the 63.2th percentile is replaced with design life, L_D, given at design failure probability, P_D. As a consequence, the theory is focused on a conservatively-low percentile of times to failure (in particular on the 1st, see below): this is both more correct from the viewpoint of modern probabilistic design of power components and on the safe side as for power component reliability [5]. Furthermore, the whole theory is formalized more extensively and carefully, with a more detailed treatment of the

effect of current harmonics and of a possible increase of thermal and electric stress associated with the sinusoidal components of voltage and current.

From the applicative viewpoint, a first novelty compared to previous papers is the treatment of both the 5th, 7th, 11th, 13th voltage harmonics already studied in [9], and of the 17th, 19th, 23rd, 25th, tackled here for the first time. Such harmonics are characteristic of 6-pulse—some of them of 12-pulse—alternating/direct current (AC/DC) converters; they play a major role, since are not only the highest in the spectra of voltage and current harmonics typically measured at the bus-bars of MV/LV grids [31,32], but also those for which Standards IEC 61000 and EN50160 set limits [2–4].

Another applicative novelty is that in our previous papers and in the existing literature the calculations were concentrated on the MTTF (design life itself was given as the design value of the MTTF) and only a spot estimation of reliability was carried out at a service time equal to design life [8,9]; moreover, the amplitudes of voltage harmonics were selected so as to match the limits in [4] exactly, only. Here, on the contrary—consistently with what is said above—the calculation is focused on the $100 \times P_D$th percentile of times to failure, and for failure probability a conservatively-low value $P_D = 0.01 = 1\%$ is chosen to be on the safe side as for power component reliability. One more novelty is that, pragmatically, design life L_D of power components is the typical service life of power systems affected by harmonics where the components are located. In addition, as for reliability estimation, reliability is evaluated throughout the service life of power components. Regarding the selected amplitude of voltage harmonics, beside the case where the amplitudes of voltage harmonics match the limits after EN 50160 exactly, two more cases are considered where voltage harmonics are 25% above and 25% below the limits in [4], so as to illustrate respectively the problems that may arise if these limits are overcome and the problems which may still remain even if these limits are matched with an apparently-broad safety margin—e.g., resorting to passive and/or active filters [31].

As a last, but not least applicative novelty-as hinted at above—two more components of power systems, i.e., induction motors and MV/LV transformers, are studied here in the presence of harmonics from power electronic converters in addition to cables and capacitors, already studied in the previous stages of this investigation.

On the whole, it is worth emphasizing that the calculations in this paper are completely new compared with those in previous ones [8,9], that have intentionally been cited here to allow a direct comparison. As highlighted hereafter at Section 3 in comprehensive tables for the cable and the capacitor, as well as for the motor and the transformer, such a comparison shows that all results and figures in this paper—although being intentionally homologous to those in previous papers for enabling a straightforward comparison—are not only different as for the values obtained and the curves plotted, but also on the safe side with respect to those in [8,9]. This highlights the need for the more accurate analysis performed for the first time in this paper vs. the simpler one carried out in previous papers. This overall comparison is also opportune in a Special Issue paper, which can take the chance for reviewing and completing previous investigations so as to outline the state of the art and the ultimate achievements in this field.

Last but not least, an aspect to mention as a closure of this Introduction is that—as hinted at above—similar models were also used focusing on the effect of either current harmonics on thermal aging as in [33,34], or voltage harmonics on electrical aging as in [35,36], with results which agree with those found in this investigation. However, the full application to electrical and thermal aging of insulation in under current and voltage harmonics has been carried out only in the streamline of the development and refinement of the electro-thermal reliability model used here, which finds in this paper its conclusive application.

2. Theoretical Background of Insulation Aging in the Presence of Voltage and Current Harmonics

The weakest part of a power system component is mostly its insulation [37]. In the presence of the harmonic distortion generated by a power electronic device, a reduction of insulation life at a given

failure probability—or, conversely, of insulation reliability at a given service time—may be observed vs. rated sinusoidal life and/or reliability due to a possible rise of [6,7]:

1.　temperature, which involves an increase of the thermal stress. Indeed, current harmonics in the conducting parts and voltage harmonics in the dielectrics may warm up the insulation. In the following, only the increase of temperature due to harmonic currents is considered, while the warming-up effect of voltage harmonics is neglected. Indeed, the main applications here are conceived for MV and LV systems (see Section 3), where dielectric losses are negligible;
2.　electric stress, associated with the non-sinusoidal voltage waveshape.

Let us now treat cases 1 and 2 separately (Sections 2.1 and 2.2), then combine them (Section 2.3) and later on recast them into a probabilistic time-varying framework (Sections 2.4 and 2.5).

2.1. The Role Played by Current Harmonics

Treating case 1 of Section 2 first, let us assume that a power electronic device generates M current harmonics (of root mean square (rms) value I_h, $h = 1, \ldots, M$), and that such current harmonics lead to a non-negligible increase (current harmonics superimposed to fundamental current can only increase the losses in conducting parts, thus the temperature of the component. Of course, such an increase might be negligible, i.e., non-measurable.) ΔT_{arm} of the temperature (herein, all temperatures T are meant in K, while the corresponding temperatures in degrees Celsius are indicated as θ) of the insulation of a nearby power component. Let us further hypothesize that the temperature of the insulation of the affected component increases from the nominal–design–sinusoidal temperature T_S to a "non-sinusoidal" temperature T_{NS} equal to:

$$T_{NS} = T_s + \Delta T_{arm} \tag{1}$$

Then, the following thermal life model can be used for the estimation of the time to failure of the insulation of the power component in the presence of the M current harmonics generated by the power electronic device and affecting the component [6–9]:

$$L_{NS,I} = L_S exp(-B\Delta T'_{harm}) \tag{2}$$

where:

- $L_{NS,I}$ = insulation time-to-failure (life) in the presence of non-sinusoidal current I_{NS}, thus of non-sinusoidal temperature T_{NS};
- L_S = life at nominal–design–sinusoidal current (of rms value I_S) and voltage (of rms value V_S), thus in the presence of design values of temperature T_S and electric field E_S (a trivial geometrical proportionality factor relates design electric field E_S to design voltage V_S, as well as non-sinusoidal electric field E_{NS} to non-sinusoidal voltage V_{NS} (see Section 2.2.));
- $B = \Delta W/k_B$ is the well-known parameter typical of the Arrhenius thermal life model, being ΔW the activation energy of the main thermal degradation reaction and k_B the Boltzmann constant [38,39];
- $\Delta T'_{harm}$ = a quantity depending on ΔT_{arm} and equal to (see Equation (1)):

$$\Delta T'_{harm} = \frac{1}{T_S} - \frac{1}{T_{NS}} = \frac{1}{T_S} - \frac{1}{(T_S + \Delta T_{arm})} \tag{3}$$

From (3) it is readily seen that the greater the increase ΔT_{arm}—if any—of the temperature of the insulation, the shorter is life in the presence of current harmonics.

Of course, the use of model (2) requires that the relationship between the M current harmonics and the relevant variation ΔT_{arm} of the temperature of the insulation is known.

2.2. The Role Played by Voltage Harmonics

Coming now to case 2 of Section 2, let us assume that a power electronic device generates N voltage harmonics (of rms value V_h, $h = 1, \ldots, N$), and that such voltage harmonics distort non-negligibly the nominal–design–sinusoidal voltage waveshape at power frequency applied to the insulation of a nearby component connected to the AC power grid. The distortion is said to be "non-negligible" if at least one of the three following quantities associated with the distorted voltage waveshape change sensibly (i.e., in a measurable way) from their nominal sinusoidal value:

1. the rms value of voltage, which changes from the nominal sinusoidal rms value $V_S = V_{1,n}$ (rms nominal sinusoidal voltage of harmonic order $h = 1$ or rms fundamental voltage at power frequency (For components connected directly to the AC power grid, the frequency of the fundamental harmonic f_1 coincides with the power frequency, $f_0 = 50/60$ Hz.)) to V_{NS}, the rms value of distorted voltage. Then, the rms value of distorted voltage in p.u. of the rms value of rated sinusoidal voltage, v_{NS}, can be written as follows:

$$v_{NS} = \frac{V_{NS}}{V_S} = \frac{V_{NS}}{V_{1,n}} \tag{4}$$

2. the peak value of voltage, which changes from the peak value of the nominal sinusoidal voltage $V_{S,p} = V_{1,n,p}$ to $V_{NS,p}$, the rms value of distorted voltage. Then, the peak value of distorted voltage in p.u. of the peak value of rated sinusoidal voltage, $v_{NS,p}$, can be written as follows:

$$v_{NS,p} = \frac{V_{NS,p}}{V_{S,p}} = \frac{V_{NS,p}}{V_{1,n,p}} \tag{5}$$

3. the rms value of the derivative of voltage, which changes from the rms value of the derivative of nominal sinusoidal voltage $hV_{1,n} = V_{1,n}$ to the rms value of the derivative of distorted voltage, where N different voltage harmonics of order h are now present. Then, by defining the ratio "rms value of the hth voltage harmonics" over "rms fundamental voltage at power frequency" $\alpha_h = V_h/V_{1,n}$, the rms value of the derivative of each of these voltage harmonics in p.u. of the rms value of nominal sinusoidal voltage can be written as follows:

$$hV_h/V_{1,n} = h\alpha_h \tag{6}$$

The distortion of the voltage waveshape, in turn, may result in an increase of the electric stress acting on the insulation of the power component. Such increase—if any—is due to the distorted electric field (of rms value E_{NS}) within the insulation caused by the non-sinusoidal voltage (of rms value V_{NS}). The increase of the electric stress in distorted regime is quantified by the so-called "voltage waveshape factors", which can be defined from Equations (4)–(6) as follows [6–10]: peak factor:

$$K_p = v_{NS,p} \tag{7}$$

waveshape factor (or slew rate) (If—differently from here—one wants to study the reliability of the insulation of a component not directly connected to the AC power grid—e.g., a PWM inverter controlling a three-phase motor whose working frequency f_1 is different from power frequency f_0, then the frequency of the fundamental harmonic is f_1 and the ratio f_1/f_0 should appear as a multiplying factor of the right-hand side of Equation (8)):

$$K_w = \sqrt{\sum_{h=1}^{N} h^2 \alpha_h^2} \tag{8}$$

rms factor:

$$K_r = v \tag{9}$$

Equations (7)–(9) clearly demonstrate that, when nominal sinusoidal voltage is applied, the three voltage waveshape factors are equal to unity, namely $K_p = K_w = K_r = 1$. By contrast, when N voltage harmonics are superimposed onto nominal sinusoidal voltage, it is observed that:

(a) K_p can be either greater or lower than 1, depending on the phase-shift angle ϕ_h between the voltage harmonics V_h and the fundamental V_1. Typically, the peak factor affects insulation life at most among the voltage waveshape factors, as made clear in Section 3 [8,9,35].
(b) K_w and K_r are always greater than 1, being definite positive quantities with lower value equal to 1, but the higher are the values of N and V_h, the higher are the values of K_w and K_r, and the more distorted is the voltage waveshape. This observation is consistent with the definition of the total harmonic distortion factor of the voltage, THD_V, related to K_w as follows [2–4]:

$$THD_v = \sqrt{\sum_{h=2}^{N} h^2 \alpha_h^2} = \sqrt{K_w^2 - 1} \tag{10}$$

Then, the following electrical life model can be used for the estimation of the time to failure of the insulation of a power component in the presence of the N voltage harmonics generated by the power electronic device [6–10]:

$$L_{NS,V} = L_S K_p^{-n_p} K_w^{-n_w} K_r^{-n_r} \tag{11}$$

where:

- $L_{NS,V}$ = insulation time-to-failure (life) under non-sinusoidal voltage/field, V_{NS}/E_{NS}, but at nominal—design—sinusoidal current I_S, thus in the presence of design temperature T_S;
- L_S = same as in Equation (2), namely life at nominal sinusoidal current I_S and voltage V_S, thus in the presence of design values of temperature T_S and electric field E_S;
- n_p = exponent that accounts for the aging acceleration effect of K_p, if any [35];
- n_w = exponent that accounts for the aging acceleration effect of K_w;
- n_r = exponent that accounts for the aging acceleration effect of K_r.

From Equation (11) it is readily seen that the greater the values of K_p, K_w, K_r with respect to unity, the shorter is life in the presence of voltage harmonics. However, it must be highlighted that—as pointed out above and in [36]—it is not granted that a distorted voltage waveshape necessarily leads to a value of $K_p > 1$, as clearly shown in Section 3.

2.3. The Combination of Current and Voltage Harmonics

When a power system component is subjected to both current and voltage harmonics generated by a power electronic device, then a combination of the life models (2) and (11) is required for a thorough and complete evaluation of the effect of distorted current and voltage on the life of the component. By combining these models, the following electro-thermal life model for distorted conditions is obtained:

$$L_{NS} = L_S exp(-B\Delta T'_{harm}) K_p^{-n_p} K_w^{-n_w} K_r^{-n_r} \tag{12a}$$

where L_{NS} is insulation life in the presence of non-sinusoidal voltage, V_{NS}, and non-sinusoidal temperature T_{NS}.

A careful analysis of Equations (4)–(11) emphasizes that voltage waveshape factors K_p, K_w, K_r are defined with respect to nominal sinusoidal voltage, hence life models (11) and (12) implicitly assume that the fundamental component of the distorted voltage waveshape (of rms value V_1) is equal to the rated sinusoidal voltage (of rms value $V_S = V_{1,n}$). However, it might happen that the fundamental

component of distorted voltage has rms value V_H higher-than-rated sinusoidal voltage V_S, for instance because a highly capacitive load—e.g., a capacitor bank—is also supplied by the voltage source (only an increase of sinusoidal voltage is considered, since a lower than rated sinusoidal voltage is not common in unperturbed conditions, even under full inductive load; moreover considering a decrease of sinusoidal voltage is not on the safe side as for the estimation of life and reliability of power components). This situation tends to reduce the life of the insulation of power components with respect to nominal sinusoidal life, too: not because of voltage harmonics, but because a higher-than-rated sinusoidal electric field, E_H, is applied to the insulation. Such an effect has to be accounted for, resorting to the well-known Inverse Power Law electrical life model (IPM), that can be written as follows:

$$L_H = L_S (E_H/E_S)^{-n_S} \tag{12b}$$

where:

- L_H = insulation life in the presence of higher-than-rated non-sinusoidal voltage/field, V_H/E_H, and sinusoidal temperature T_S;
- n_S = the so-called life exponent or voltage endurance coefficient, that rules the life variation due to a change of sinusoidal voltage/field compared to design sinusoidal voltage/field [38,39].

Thereafter, by combining Equations (12a) and (12b), one obtains the following comprehensive life model:

$$L_{NS} = L_S (E_H/E_S)^{-n_S} exp(-B\Delta T'_{harm}) K_p^{-n_p} K_w^{-n_w} K_r^{-n_r} \tag{13}$$

In addition, when looking carefully at Equations (1)–(3) it can be argued that non-sinusoidal temperature T_{NS} is defined with respect to nominal sinusoidal temperature T_S, hence life models (2), (12) and (13) implicitly assume that the fundamental component of the distorted current waveshape (of rms value I_1)—let us call it "sinusoidal current"—is equal to the rated sinusoidal current (of rms value $I_S = I_{1,n}$). However, it might happen that the fundamental component of distorted current has rms value I_{HL} higher/lower than rated sinusoidal current I_S, for instance due to a temporary overload/underload—e.g., because linear loads demand a higher/lower-than-rated current. This situation tends to reduce/increase the life of the insulation of the power component with respect to nominal sinusoidal life, too: not because of current harmonics, but because a higher/lower-than-rated "sinusoidal" temperature, T_{HL}, is applied to the insulation. If this is the case, let us write T_{HL} as follows:

$$T_{HL} = T_S + \Delta T_{HL} \tag{14a}$$

where ΔT_{HL} is higher/lower than zero depending on whether linear loads demand a higher/lower-than-rated current. Moreover, let us introduce the overall temperature variation ΔT_{tot} with respect to nominal sinusoidal temperature T_S resulting from:

- the temperature variation caused by harmonic currents, ΔT_{arm};
- the temperature variation caused by a change of sinusoidal current with respect to rated sinusoidal current, ΔT_{HL}.

Thus ΔT_{tot} can be written as follows:

$$\Delta T_{tot} = T_S + \Delta T_{arm} + \Delta T_{HL} \tag{14b}$$

and a quantity $\Delta T'_{tot}$—analogous to $\Delta T'_{trm}$ defined in Equation (3)—can be introduced, as follows:

$$T'_{tot} = 1/T_S - 1/(T_S + \Delta T_{arm} + \Delta T_{HL}) = 1/T_S - 1/(T_S + \Delta T_{tot}) \tag{15}$$

Therefore, by combining Equation (13) with Equations (14)–(15) one obtains the following electro-thermal life model holding in the presence of voltage and current harmonics, as well as of higher-than-rated sinusoidal voltage and current [9]:

$$L_{NS} = L_S(E_H/E_S)^{-n_S} exp(-B\Delta T'_{tot})K_p^{-n_p} K_w^{-n_w} K_r^{-n_r} \tag{16}$$

Model (16) is a comprehensive relationship which accounts for:

- a possible higher-than-rated sinusoidal electric field/voltage, $E_H > E_S/V_H > V_S$;
- a possible higher/lower than rated sinusoidal temperature, $T_{HL} > T_S/T_{HL} < T_S$, caused by a higher/lower than rated sinusoidal current, $I_{HL} > I_S/I_{HL} < I_S$;
- a distorted current due to M voltage harmonics, which causes an increase ΔT_{arm} of temperature with respect to rated sinusoidal temperature;
- a distorted voltage due to N voltage harmonics, which causes a change of voltage waveshape with respect to rated sinusoidal voltage.

2.4. Reliability Model in the Presence of Current and Voltage Harmonics

The electro-thermal breakdown of the insulation of a power component is an inherently random phenomenon. This is due first and foremost to the non-uniform composition of the dielectric material which constitutes the insulation, as well as to the randomly distributed defects within the insulation itself. A further reason for the random behavior of insulation breakdown is the uncertainty of the values of applied electrical and thermal stress [40,41]. For these reasons, all the above models—and in particular the general electro-thermal life model (16) holding in the presence of voltage and current harmonics—have to be recast into a probabilistic framework, whereby life (time to failure) of insulation is a random variable associated with a certain failure probability. This requires the introduction of a proper probability distribution of failure times. As is well known, failure statistics in polymeric insulation fit well the Weibull probability distribution [5,42], whereby insulation time to failure t_F can be represented by means of a 2-parameter Weibull cumulative probability distribution function (cdf) of failure times, given in the following equation:

$$P(t_F) = P = 1 - exp[-(t_F/\alpha_t)]^{\beta_t} \tag{17}$$

where P is cumulative failure probability corresponding to time to failure t_F, α_t is the scale parameter (the 63.2th percentile of the life) and β_t is the shape parameter of the Weibull probability distribution function. This means that insulation time to failure t_F is a random variable associated with a certain value of failure probability P, or—conversely—of reliability $R = 1 - P$. Equation (17) can be easily recast in terms of α_t as follows:

$$\alpha_t = t_F/[-ln(1-P)]^{1/\beta_t} \tag{18}$$

As a consequence, the reliability of a power component subjected to current and voltage harmonics can be estimated from the general model (16) by assuming that component life is Weibull-distributed according to (17). In this respect, it is worth pointing out that here—contrary to previous papers [6–9] based on the 63.2th percentile of time to failure, α_{NS}, and on the expected value of time to failure, μ_{NS}—the theory and the calculations for distorted conditions are focused on noteworthy $100 \times P$th percentiles of the Weibull distribution of times to failure in distorted conditions, $t_{P,NS}$, which are compared in the applicative section with design life in sinusoidal conditions, L_D, given at a certain cumulative failure probability, P_D: this is consistent with the modern probabilistic approach to the design of power component insulation. Therefore, in order to recast model (16) in terms of $t_{P,NS}$, L_D and P_D, the following procedure is required.

Let us first write Equation (18) twice:

1. a first time for $t_{P,NS}$, namely insulation life in non-sinusoidal conditions at a generic failure probability P, as follows:

$$P(t_{P,NS}) = P = 1 - exp[-(t_{P,NS}/\alpha_{NS})]^{\beta_t} \tag{19}$$

where α_{NS} indicates the 63.2th percentile (or scale parameter) of non-sinusoidal life distribution;

2. a second time for L_D, namely insulation life in nominal sinusoidal conditions at design failure probability P_D—indeed life is now a random variable, hence also design life L_D is associated with a certain fixed and known design failure probability, P_D, see above—as follows:

$$P(L_D) = P_D = 1 - exp[-(L_D/\alpha_S)]^{\beta_t} \tag{20}$$

where α_S indicates the 63.2th percentile (or scale parameter) of sinusoidal life distribution.

Thereafter, using Equation (18) let us explain (19) and (20) in terms of the scale parameter, as follows:

$$\alpha_{NS} = t_{P,NS}/[-ln(1-P)]^{1/\beta_t} \tag{21}$$

$$\alpha_S = L_D/[-ln(1-P_D)]^{1/\beta_t} \tag{22}$$

Considering now model (16), it is readily seen that this model has to be written for a given failure probability as well, in such a way that life in the presence of current and voltage harmonics, L_{NS} (at the left-hand side) and sinusoidal life L_S at the right-hand side are relevant to the same failure probability: indeed, L_{NS} at the left-hand side and L_S at the right-hand side are so far the only random variables in model (16) (for the moment, K_p, K_w and K_r are assumed as deterministic and known, since the N voltage harmonics are assumed as deterministic and known so far. In the following, also the typical random variation of harmonics is accounted for). Therefore, model (16) can be written, e.g., for 63.2% failure probability, so that $L_{NS} = \alpha_{NS}$ and $L_S = \alpha_S$. In this way, one obtains:

$$\alpha_{NS} = \alpha_S (E_H/E_S)^{-n_S} exp(-B\Delta T'_{tot}) K_p^{-n_p} K_w^{-n_w} K_r^{-n_r} \tag{23}$$

Then, by expressing α_{NS} via (21) and α_S via (22), relationship (23) becomes:

$$\frac{t_{P,NS}}{[-ln(1-P)]^{1/\beta_t}} = \frac{L_D}{[-ln(1-P_D)]^{1/\beta_t}} (E_H/E_S)^{-n_S} exp(-B\Delta T'_{tot}) K_p^{-n_p} K_w^{-n_w} K_r^{-n_r} \tag{24}$$

which can be eventually recast in the following form—reported here for the first time:

$$t_{P,NS} = L_D \frac{[-ln(R)]^{1/\beta_t}}{[-ln(1-P_D)]^{1/\beta_t}} (E_H/E_S)^{-n_S} exp(-B\Delta T'_{tot}) K_p^{-n_p} K_w^{-n_w} K_r^{-n_r} \tag{25}$$

Relationship (25) is the so-called electro-thermal "probabilistic life model"—or "reliability model"—for the insulation of a power component affected by current and voltage harmonics. It is a quite powerful tool that, for given values of design life L_D and design failure probability P_D, relates the $100 \times P$th percentile of insulation time-to-failure (life) in non-sinusoidal regime, $t_{P,NS}$, to reliability $R = 1 - P$ and applied stresses, i.e., temperature associated with linear and no linear loads, sinusoidal voltage and voltage waveshape factors. Therefore, this relationship yields the main functions and parameters needed for a thorough reliability analysis of power system components, namely [8]:

Reliability function

$$R(t_{P,NS}) = exp\left\{ -\left\{ \frac{[-ln(1-P_D)]^{1/\beta_t} t_{P,NS}}{L_D(E_H/E_S)^{-n_S} exp\left(-B\Delta T'_{tot}\right) K_p^{-n_p} K_w^{-n_w} K_r^{-n_r}} \right\}^{\beta_t} \right\} \tag{26}$$

Failure probability

$$P(t_{P,NS}) = 1 - R(t_{P,NS}) \tag{27}$$

Hazard function

$$h(t_{P,NS}) = \frac{[-ln(1 - P_D)]^{1/\beta_t} \beta_t (t_{P,NS})^{\beta_t - 1}}{\left\{ L_D (E_H / E_S)^{-n_S} exp\left(-B\Delta T'_{tot}\right) K_p^{-n_p} K_w^{-n_w} K_r^{-n_r} \right\}^{\beta_t}} \tag{28}$$

Mean Time To Failure (MTTF)

$$MTTF = \frac{L_D}{[-ln(1 - P_D)]^{1/\beta_t}} (E_H / E_S)^{-n_S} exp\left(-B\Delta T'_{tot}\right) K_p^{-n_p} K_w^{-n_w} K_r^{-n_r} \Gamma(1 + 1/\beta_t) \tag{29}$$

where Γ is the Euler Gamma function.

2.5. Reliability Model in the Case of Randomly Time-Varying Distortion

Voltage and current harmonics have amplitude and phase-angle that are stochastically varying with time. Therefore, they have to be regarded as random variables (RVs), in line with [4] and as done hereafter from both the theoretical and the applicative viewpoint.

If the probability density functions (pdfs) of voltage and current harmonics at a certain node of the grid are known, life and reliability of power components at that node can be inferred by applying the cumulative damage law of Miner [43] to the reliability model (25). Then, the following probabilistic electrothermal life model for randomly time-varying distortion is obtained:

$$t_{P,NS} = \frac{[-ln(R)]^{1/\beta_t}}{\int_0^{I_{1,max}} \cdots \int_0^{I_{M,max}} \int_0^{V_{1,max}} \cdots \int_0^{V_{N,max}} \cdots \dfrac{f(I_1, ..., I_N; V_1, ..., V_N) \prod_{h=1}^N dV_h \prod_{h=1}^M dI_h}{\dfrac{L_D}{[-ln(1-P_D)]^{1/\beta_t}} \left(\dfrac{E_H}{E_S}\right)^{-n_S} exp(-B\Delta T'_{tot}) K_p^{-n_p} K_w^{-n_w} K_r^{-n_r}}} \tag{30}$$

where: $f(I_1, \ldots, I_M; V_1, \ldots, V_N)$ is the multivariate pdf of rms current harmonics ($I_1, .., I_M$) and rms voltage harmonics ($V_1, \ldots, V_N$); $I_{1,max}, .. I_{M,max}$ and $V_{1,max}, .. V_{N,max}$ are, respectively, the maximum values reached with time by rms harmonic currents and voltages. It must be emphasized that in LV and MV systems ΔT_{arm}—thus $\Delta T'_{tot}$, see Equation (15)—depends directly on the amplitudes of current harmonics only (Dielectric losses are practically negligible in LV and MV systems.), while K_p, K_w and K_r depend directly on the amplitude and phase of voltage harmonics (the dependence on the phases of voltage harmonic is omitted in (30) for the sake of simplicity).

Let us now assume that the temperature variation caused by harmonic currents, ΔT_{arm}, and the temperature variation caused by a change of sinusoidal current with respect to rated sinusoidal current, $\Delta T_{HL,}$ can be regarded as constant with time, since temperature exhibits moderate fluctuations of a few K around a mean value $\langle T_{tot} \rangle$ which is essentially constant in the rms sense [2,3]. Then $\langle T_{tot} \rangle$ can be essentially regarded as a deterministic quantity, constant with time in the rms sense as well; this means that the thermal effects of currents can be also essentially regarded as deterministic. As a consequence, (30) can be made much simpler, as follows:

$$t_{P,NS} = \frac{\dfrac{L_D [-ln(R)]^{1/\beta_t}}{[-ln(1-P_D)]^{1/\beta_t}} \left(\dfrac{E_H}{E_S}\right)^{-n_S} exp(-B\langle \Delta T'_{tot} \rangle)}{\int_0^{K_{p,max}} \int_0^{K_{w,max}} \int_0^{K_{r,max}} \dfrac{f(K_p, K_w, K_r) dK_p dK_w dK_r}{K_p^{-n_p} K_w^{-n_w} K_r^{-n_r}}} \tag{31}$$

where:

- $f(K_p, K_w, K_r)$ is the multivariate pdf of K_p, K_w and K_r, correlated in turn with $f(V_1, .., V_N; \phi_1, \ldots, \phi_N)$, the multivariate pdf of rms values, $V_1, .., V_N$, and phase-shift angles $\phi_1, \ldots, \phi_N$ of voltage harmonics;

- $\langle \Delta T'_{tot} \rangle$ is defined as follows (see Equation (15)):

$$\langle \Delta T'_{tot} \rangle = 1/T_S - 1/(T_S + \langle \Delta T_{arm} + \Delta T_{HL} \rangle) = 1/T_S - 1/(T_S + \langle \Delta T_{tot} \rangle) \tag{32}$$

Equation (31) can be rewritten in a more compact form as follows:

$$t_{P,NS} = \frac{L_D[-ln(R)]^{1/\beta_t}(E_H/E_S)^{-n_S}exp(-B\langle \Delta T'_{tot} \rangle)}{[-ln(1-P_D)]^{1/\beta_t}\, E\left[K_p^{n_p} K_w^{n_w} K_r^{n_r}\right]} \tag{33}$$

where $E\left[K_p^{n_p} K_w^{n_w} K_r^{n_r}\right]$ indicates the expected value of $K_p^{n_p} K_w^{n_w} K_r^{n_r}$.

The above hypothesis that ΔT_{arm} and ΔT_{HL} can be regarded as constant with time is meaningful, particularly as far as ΔT_{arm} is concerned [2,3]. Indeed, load current does vary with time, but the associated variation of Joule losses is more or less compensated by the thermal inertia of the insulation of the component and of the surrounding environment, which have a much longer thermal time constant than the typical variation period of harmonic currents—and sometimes even of sinusoidal current. Therefore, the overall thermal effect of load current can be well approximated as a steady variation of the temperature of the component, proportional to rms load current (the use of rms current is due to the dependence of Joule losses in conducting parts on the rms value of current).

Then, from Equation (33) it follows that life and reliability of the insulation of the component affected by harmonic distortion can be estimated in two steps:

1. evaluation of the $100 \times P$th failure time percentile based on the effect of voltage harmonics only, $t_{P,NS,V}$, resorting to the following equation (derived from Equation (33) by setting $\langle \Delta T'_{tot} \rangle = 0$, which implies $exp(-B\langle \Delta T'_{tot} \rangle) = 1$):

$$t_{P,NS,V} = \frac{L_D[-ln(R)]^{1/\beta_t}(E_H/E_S)^{-n_S}}{[-ln(1-P_D)]^{1/\beta_t}E\left[K_p^{n_p} K_w^{n_w} K_r^{n_r}\right]} \tag{34}$$

2. evaluation of the further possible variation of the $100 \times P$th failure time percentile due to the effect of the mean value of $\Delta T'_{tot}$, $\langle \Delta T'_{tot} \rangle$—guessed in turn through rms load current—resorting to the following equation, derived comparing Equation (33) with Equation (34):

$$t_{P,NS} = t_{P,NS,V}\, exp(-B\langle \Delta T'_{tot} \rangle) \tag{35}$$

Focusing on the 1st step, a proper application of Equation (34) requires an appropriate description of the time variation of voltage harmonics. This variation is inherently stochastic, but two typical situations can occur at a certain node of a grid where a component of interest is located:

(I) a monitoring survey has provided m values of the amplitudes and phases of voltage harmonics measured throughout a time interval t_m, which on the one hand should be as long as possible to well describe component duty service, but on the other hand is restricted by practical constraints, e.g., 1 h, 1 day, 1 week [4]. Monitored data like these are rarely found [7,32,35,36], but if they are available they enable the straightforward computation of the values of K_p, K_w, K_r through Equations (7)–(9) and derivation of the relevant sampling distribution, which is the numerical reproduction of the multivariate pdf $f(K_p, K_w, K_r)$—see [7].

(II) the pdfs of voltage harmonics can be guessed analytically according to a parametric approach. Then, $f(V_1,..,V_N; \phi_1, \dots, \phi_N)$ is readily available, whereby in turn $f(K_p, K_w, K_r)$ can be derived.

In both cases, once the multivariate pdf $f(K_p, K_w, K_r)$ has been obtained, the life and reliability of the power component subjected to randomly time-varying voltage harmonics can be evaluated by means of Equation (34) by computing the expected value $E\left[K_p^{n_p} K_w^{n_w} K_r^{n_r}\right]$.

Coming to the 2nd step, the further effect of time-varying current harmonics—involving in turn a constant (in the rms sense) variation of insulation temperature $\langle \Delta T'_{tot} \rangle$—can be assessed by means of Equation (35).

Since the focus in this paper is on the 1st percentile of times to failure in the presence of harmonic distortion, $t_{1\%,NS}$, its calculation requires rewriting Equation (33) for $R = R_D = 0.99$ (i.e., $P_D = 0.01$), namely:

$$t_{1\%,NS} = \frac{L_D exp(-B\langle \Delta T'_{tot} \rangle)(E_H/E_S)^{-n_S}}{E\left[K_p^{n_p} K_w^{n_w} K_r^{n_r}\right]} \tag{36}$$

Moreover, reliability is calculated as a function of time elapsed in service, t_E, by explaining Equation (33) as a function of R with R_D set to 0.99, as follows:

$$R(t_E) = exp\left\{-\left\{\frac{[-ln(0.99)]^{1/\beta_t} t_E E\left[K_p^{n_p} K_w^{n_w} K_r^{n_r}\right]}{L_D(E_H/E_S)^{-n_S} exp\left(-B\langle \Delta T'_{tot} \rangle\right)}\right\}^{\beta_t}\right\} \tag{37}$$

By setting $\langle \Delta T'_{tot} \rangle = 0$ in (36), (37), homologous relationships valid in the presence of voltage harmonics only are obtained, i.e.,:

$$t_{1\%,NS} = L_D(E_H/E_S)^{-n_S} / E\left[K_p^{n_p} K_w^{n_w} K_r^{n_r}\right] \tag{38}$$

$$R(t_E) = exp\left\{-\left\{[-ln(0.99)]^{1/\beta_t} t_E E\left[K_p^{n_p} K_w^{n_w} K_r^{n_r}\right]/\left[L_D(E_H/E_S)^{-n_S}\right]\right\}^{\beta_t}\right\} \tag{39}$$

The reliability model for time-varying distortion as newly formulated here relies on Equations (38) and (39) or (36) and (37)—depending on whether $\langle \Delta T'_{tot} \rangle = 0$ or $\neq 0$, respectively—which differ from those used in [8,9], since these latter are based on the 63.2th percentile of failure time. For the sake of simplicity, hereafter the sinusoidal component of electric field at power frequency is taken equal to rated sinusoidal electric field, namely $E_H = E_S$.

3. Application of the Reliability Model for Randomly Time-Varying Distortion

3.1. Selected Case Studies

In previous papers [8,9] the reliability model for randomly time-varying distortion was applied to power system components affected by voltage harmonics whose amplitudes matched the limits after EN 50160 [4] exactly. The calculations were concentrated on the 63.2th percentile of time to failure, α_{NS}, and on the mean time to failure (MTTF), μ_{NS}; design life itself was given as the design value of the MTTF in sinusoidal conditions set to 40 and 30 years for the cable and the capacitor, the two treated components. Reliability was estimated at a service time equal to design life only.

Here, the calculations are focused on the $100 \times P_D$th percentile of times to failure, which is consistently compared with design life in sinusoidal conditions, L_D, given at design failure probability $P_D = 0.01 = 1\%$. This is in line with the modern probabilistic design of the insulation of power components, which requires high reliability [5]. Moreover, the design life of power components is set pragmatically to $L_D = 20$ years, i.e., the typical order of magnitude of the service life (based on the duration of the mortgages and the amortization times) of industrial plants, traction systems for railways or subways and renewable power plants for photovoltaic (PV) and wind energy generation [44–46]. Grid-connected three-phase power electronic converters are found to connect these plants with the AC power grid and they generate voltage and current harmonics which affect nearby components. This has the first and foremost effect that all estimates obtained here for failure time percentiles and reliability are different from those in previous papers.

In addition, in place of the "spot" reliability estimate at design life in [8,9], reliability is evaluated here in terms of design life of power components—and even beyond it, although results are omitted for brevity. Indeed, as service time t_E goes by, maintenance and/or repair and/or replacement actions

might be required on some components of the plant/grid, if their residual reliability is unsatisfactory; conversely, other components may remain in service without any action even after a service time t_E equal to—or even longer than—design life L_D, if their residual reliability is unsatisfactory. For this reason, beside proper diagnostic techniques, a sound reliability model can be extremely useful to provide indications about the residual reliability of components all along their time on duty.

Furthermore, the case studies treated in this paper have been changed and broadened considerably compared to [8,9], as shown in the next section. First of all, the voltage harmonics treated in [8] were the 11th, 13th, to which the 5th, 7th were added in [9], while here for the first time the 17th, 19th, 23rd, 25th are included. It is worth emphasizing that the implementation of the new calculations including the whole set of odd harmonics from the 5th to 25th has required a non-negligible effort for restructuring and modifying the code: analyzing the whole sequence of odd voltage harmonics from the 5th to the 25th, as done here for the first time, is all but trivial and inexpensive from the viewpoint of theoretical and computational efforts. It is also worth outlining that the reliability model (33),(36),(37) works for all harmonic orders [10], but harmonics of order $h > 25$ are neglected here since in [4] no limits are given for voltage harmonics above the 25th, as they are said to be "*usually small, but largely unpredictable due to resonance effects*".

Moreover, three cases differing as for the magnitude (In agreement with [4] let us consider for each harmonic—in place of the rms value—the "*10 min mean rms value*", called "magnitude" from now on, and indicate it simply as V_h like the rms value.) of voltage harmonics are treated here:

(i)　a case similar (remember that only here the 5th, 7th, 11th, 13th, 17th, 19th, 23rd, 25th harmonics are considered all together) to that in [8,9], where the magnitudes V_h of the treated voltage harmonics are random variables (see Equation (30)) correlated (this hypothesis is acceptable, as shown in [7] from a data set of measured voltage harmonics with phase-shift angles [32], used here as the experimental case. Amplitudes were above the limits after [4]) to each other and following a Gaussian pdf, with such mean value $\mu_h = \mu(V_h)$ and standard deviation $\sigma_h = \sigma(V_h)$ that the 95th percentile of V_h of each harmonic matches the limits set in Tables 1 and 4 of Standard EN 50160 [4] exactly. As pointed out in [8,9], the Gaussian pdf was chosen mainly as it is a good approximation of several other pdfs [47] and it is the most practical to reproduce measured values of randomly-varying quantities such as harmonic voltages [32].

(ii)　a new case, where the Gaussian pdfs of the magnitudes V_h of voltage harmonics have such values of μ_h and σ_h that the limits in EN 50160 are exceeded by 25%, so as to illustrate the problems that may arise if these limits are overcome (e.g., in a plant without passive or active filters);

(iii)　another new case, where the Gaussian pdfs of V_h have such values of μ_h and σ_h that the limits in EN 50160 are matched with a 25%-safety margin, so as to show that problems may still remain even if limits are matched with a seemingly-broad safety margin.

Three more applicative novelties compared to previous papers [8,9] of this investigation are:

-　in addition to $<\Delta\theta_{tot}> = 0$, the case $<\Delta\theta_{tot}> = -15\,°\text{C}$—a value in between those treated in [8,9], i.e., −10 and −20 °C—is considered in order to account for the effect of current harmonics;

-　the chosen value of the shape parameter of Weibull distribution is 2 instead of 3 used in [8,9], as explained hereafter;

-　as hinted at in the Abstract and Introduction, two more components of power systems, i.e., induction motors and MV/LV transformers, are treated here in addition to cables and capacitors, already studied in the previous stages of this investigation.

As for the magnitude of voltage harmonics, it can be argued that, anyway, the reference case for setting the correct values of μ_h and σ_h in cases (i)–(iii) above is case (i). Since measurements of harmonic voltages that match the probabilistic limits set in [4] exactly are rare in the literature, the random magnitudes of harmonic voltages matching the limits set in [4] exactly are derived here via a heuristic parametric approach [8,9] based on a priori hypotheses about the Coefficient of Variation $CV_h = \sigma_h/V_h$

of harmonic voltages. Namely, two different values of CV_h are hypothesized so as to reproduce a narrower and a broader spread of V_h:

(1)　$CV_{h,1} = 0.1$, i.e., 10% of the mean of V_h;
(2)　$CV_{h,2} = 0.3$, i.e., 30% of the mean of V_h.

　　These values of CV_h were already chosen in [8,9] for the 5th, 7th, 11th, 13th voltage harmonics, being consistent with those measured in the power supply grid of a subway traction system, where CV_h ranged from ≈10% to ≈27% [32]. They are kept here and extended to the 17th, 19th, 23rd, 25th voltage harmonics, for the sake of comparison.

　　As a result of this heuristic parametric approach, the pdfs (the pdfs describing the randomness of the parameters V_h in Figure 1, as well as the one of other parameters, e.g., K_p and K_w, may be also considered as the "a priori" pdfs in a Bayesian inference framework, which is outside the scope of the present paper. The details of this approach are discussed for the problem under study in [48]) of the 5th, 7th, 11th, 13th, 17th, 19th, 23rd, 25th voltage harmonic magnitudes are obtained, which are Gaussian with μ_h and σ_h such that their magnitudes match exactly the limits set in [4], namely: 6%, 5%, 3.5%, 3%, 2.0%, 1.5%, 1.5%, 1.5% of rms fundamental voltage V_1 for the 95th percentiles of V_5, V_7, V_{11}, V_{13}, V_{17}, V_{19}, V_{23}, V_{25}, respectively [48]. The cdfs of all voltage harmonics, $F(V_h)$, are shown for the sake of illustration in Figure 1a,b for the cases $CV_{h,1} = 0.1$ and $CV_{h,2} = 0.3$, respectively: is readily seen that the limits after [4] are exactly matched for all voltage harmonics.

　　Now, life and reliability estimation according to model (36) and (37) requires knowledge of the expected value $E\left[K_p^{n_p} K_w^{n_w} K_r^{n_r}\right]$. As it can be argued from Equations (30), (31), (33), this in turn requires the knowledge of the multivariate pdf of K_p, K_w, K_r, $f(K_p, K_w, K_r)$, correlated with $f(V_5, V_7, V_{11}, V_{13}, V_{17}, V_{19}, V_{23}, V_{25}; \phi_5, \phi_7, \phi_{11}, \phi_{13}, \phi_{17}, \phi_{19}, \phi_{23}, \phi_{25})$, the multivariate pdf of magnitudes and phase-shift angles (with respect to the fundamental V_1) of the treated voltage harmonics. The derivation of the pdfs/cdfs of the magnitude of voltage harmonics (Figure 1) has solved the problem of deriving $f(V_5, V_7, V_{11}, V_{13}, V_{17}, V_{19}, V_{23}, V_{25})$, but the phase-shift angles between voltage harmonics and the fundamental is also needed to estimate the part of multivariate pdf relevant to phase-shift angles. This problem is solved—as in [8,9] for the 5th, 7th, 11th, 13th voltage harmonics—by taking phase-shift angles ϕ_5, ϕ_7, ϕ_{11}, ϕ_{13}, ϕ_{17}, ϕ_{19}, ϕ_{23}, ϕ_{25} as known deterministic quantities, both to make the treatment easier and to carry out a parametric sensitivity analysis; thereafter, $f(K_p, K_w, K_r)$ can be readily derived.

　　Such analysis focuses on three different cases (a), (b), (c) of phase-shift angles, which have quite different (or even extreme and opposite) effects on the distorted voltage waveshape. These cases are illustrated in the reference Figure 2, which shows the mean waveform of harmonic voltage pdfs for phase-shift cases (a), (b), (c) obtained using $CV_{h,1} = 0.1$ and μ_h as the magnitude of the hth harmonic in the case of exact matching of the limits after [4]. Cases (a), (b), (c) of phase-shift angles are as follows.

(a)　The sum of voltage harmonic peaks, shown in Figure 2a [49]. It is called "worst case", since it leads to the highest peak of the distorted voltage waveshape, thus to the maximum value of the peak factor K_p. The worst-case features the following set of phase-shift angles: $\phi_5 = 0$, $\phi_7 = 180°$, $\phi_{11} = 180°$, $\phi_{13} = 0$, $\phi_{17} = 0$, $\phi_{19} = 180°$, $\phi_{23} = 180°$, $\phi_{25} = 0$. In [35] the "worst case" is regarded as uncommon in a self-judged "*indicative but not exhaustive*" experimental survey. Hence it is treated here, as in [8,9], since it might happen and it is on the safe side as for the reliability analysis.

(b)　The so-called "best case", shown in Figure 2b. Indeed, it leads to the flattest distorted voltage with the lowest peak, thus to the minimum value of the peak factor K_p, namely the less prone to speed-up the degradation of the insulation. The best case features the following set of phase-shift angles: $\phi_5 = 180°$, $\phi_7 = 180°$, $\phi_{11} = 0$, $\phi_{13} = 0$, $\phi_{17} = 180°$, $\phi_{19} = 180°$, $\phi_{23} = 0$, $\phi_{25} = 0$.

(c)　The so-called "experimental case", shown in Figure 2c. This case is taken from an experimental data set—hardly found in the literature—of phase-shift angles measured on the supply system of a subway with large size (3.5 MW) 12-pulse AC/DC converters as main distorting loads, plus lower size converters and other loads generating 5th and 7th voltage harmonics [32]. The experimental case features the following set of phase-shift angles: $\phi_5 = 109°$, $\phi_7 = 300°$, $\phi_{11} = 317°$, $\phi_{13} = -15°$,

$\phi_{13} = 0$, $\phi_{17} = -16.6°$, $\phi_{19} = -17.4°$, $\phi_{23} = -19°$, $\phi_{25} = 11°$. The values of ϕ_5, ϕ_7, ϕ_{11}, ϕ_{13}, ϕ_{23}, ϕ_{25} are the mean of the measured values for these harmonics, while the values of ϕ_{17}, ϕ_{19} have been attained through a linear interpolation of the mean values of ϕ_{13} and ϕ_{23}—the 17th and 19th voltage harmonics are not found in [32]. The experimental case leads to a distorted voltage waveshape fairly similar to those observed in the field, as obvious when considering its experimental origin.
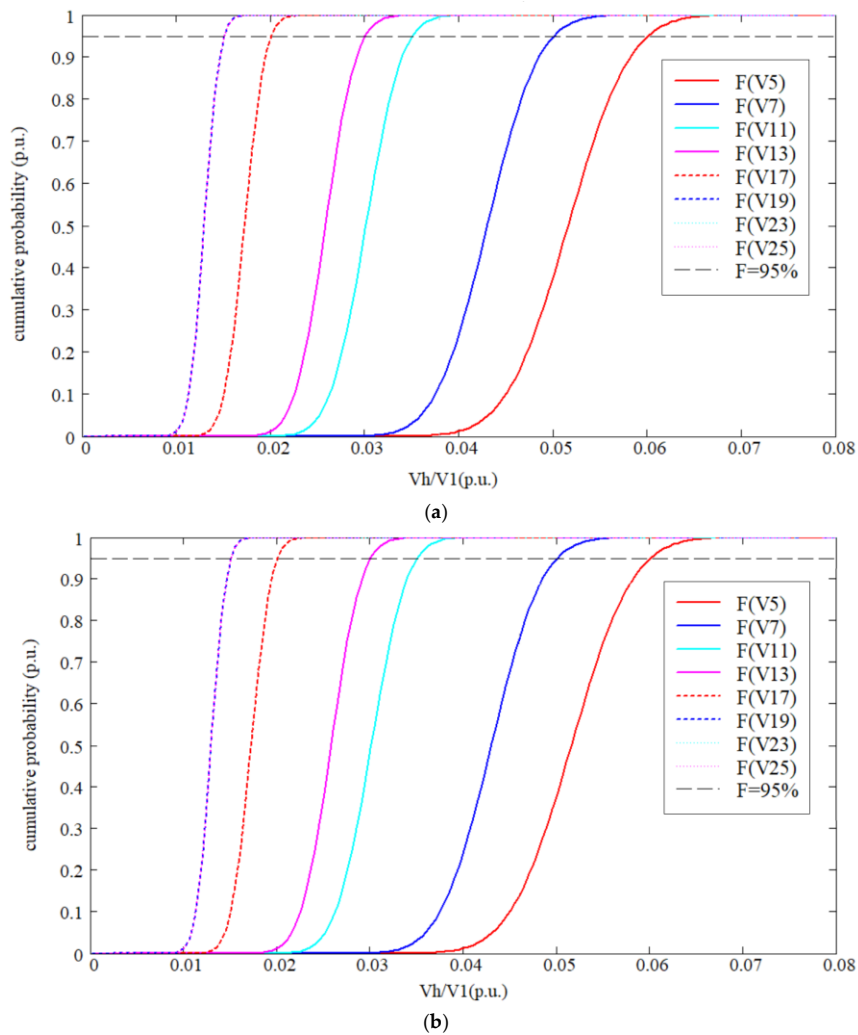

Figure 1. Gaussian cumulative distribution functions (cdfs) of the magnitudes of 5th, 7th, 11th, 13th, 17th, 19th, 23rd, 25th voltage harmonics, with μ_h and σ_h such as to match the limits in [4] exactly (6%, 5%, 3.5%, 3%, 2%, 1.5%, 1.5%, 1.5% of V_1 for the 95th percentiles): (**a**) $CV_h = 0.1$; (**b**) $CV_h = 0.3$.

Coming to the role played by current harmonics, as outlined in Section 2.5 it is assumed that ΔT_{tot} can be replaced by its mean value (in the rms sense) $<\Delta T_{tot}>$, constant with time and deterministic value. Two values of $<\Delta T_{tot}>$ are considered here, namely:

A. $<\Delta T_{tot}> = 0$ K, i.e., $<\Delta\theta_{tot}> = 0$ °C, like in [8,9], so as to emphasize the role played by voltage harmonics. Setting $<\Delta T_{tot}> = 0$ corresponds to step 1 of the procedure outlined in Section 2.5; this implies $\langle\Delta T'_{tot}\rangle = 0$, thus the reliability model (38) and (39) shall be used, focusing on the role played by voltage harmonics only. In fact, setting $<\Delta T_{tot}> = 0$ means that in practice the temperature of component oscillates, with negligible fluctuations, around design temperature;

B. $<\Delta T_{tot}> = -15$ K, i.e., $<\Delta\theta_{tot}> = -15$ °C, a value in between those treated in [8,9], i.e., −10 and −20 °C. Setting $<\Delta T_{tot}> \neq 0$ corresponds to step 2 of the procedure outlined

in Section 2.5; this implies $\langle \Delta T'_{tot} \rangle \neq 0$, thus reliability model (36) and (37) shall be used, including the role played by current harmonics and sinusoidal current. Setting a value of $<\Delta T_{tot}> < 0$ implies acknowledging that the component—notwithstanding the presence of current harmonics—works typically at a lower- than-design temperature. This holds in particular for MV distribution cables—whose design temperature oscillates between 75 °C for "vintage" paper-insulated lead-covered cables to 90 °C for extruded cables—which have usually an overall load well below the rated one [50].
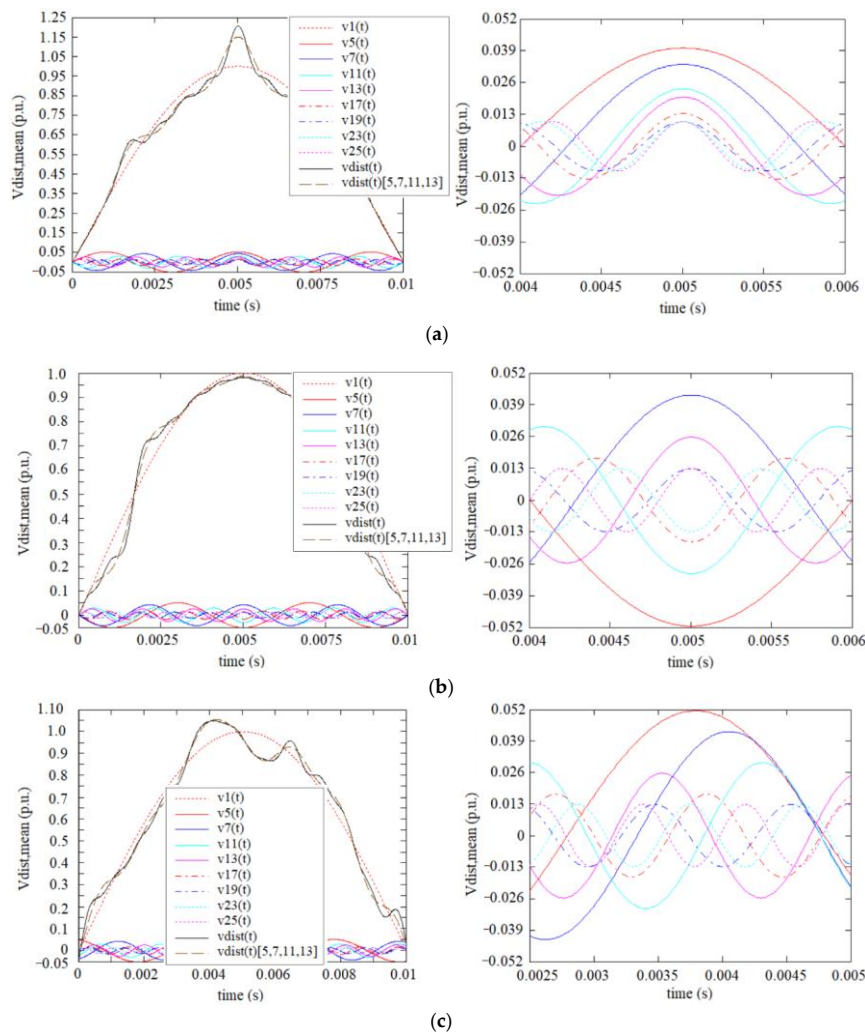
Figure 2. Mean voltage waveshapes for case studies (**a**–**c**) obtained using $CV_{h,1} = 0.1$ and μ_h as the magnitude of the hth harmonic in the case of exact matching of the limits after [4]. Left: positive halfwaves; right: zoomed-in view showing the phase-shift between harmonics. *vdist*(*t*) is total distorted voltage with all harmonics, while *vdist*(*t*) [5,7,32,38] with the 5th, 7th, 11th, 13th only as in [9]. THDv = 8.3%.

By combining above points (i)–(iii), (1)–(2), (a)–(c), A.–B., the case studies of distorted voltage waveshapes treated here are 36, as summarized in Table 1, where the relevant value of *THDv* is also reported; for making the table more compact, the cases corresponding to points (i)–(iii) above (i.e., pdfs of voltage harmonic magnitude V_h that either match the limits in [4] exactly, or overcome them by 25%, or are below them by 25%) are quoted on one single row: this implies that any one of case studies (a)–(l) degenerates in turn into three more case studies depending on the pdfs of V_h. For the sake of illustration, the mean voltage waveshapes of case studies (a), (b), (c) for the exact matching of the limits in [4] (obtained by using μ_h as the magnitude of the hth harmonics) are plotted in Figure 2a–c.

Other distorted voltage waveshapes than these may exits, but they tend to be in between those considered here, thus they tend to have intermediate effects on insulation life and reliability.

Table 1. Summary of cases of distorted voltage waveshapes studied here (interestingly, with the whole set of odd harmonics non-multiple of 3 from the 5th to the 25th, the 8% limit for THD_v after [4] is slightly overcome when $CV_h = 0.1$ even when the amplitudes of each single harmonic voltage strictly match the limits in [4]. This does not happen when 5th, 7th, 11th, 13th harmonics only are treated [9]. This is another new outcome of this study, which would deserve a deeper investigation).

Case Study	Scatter CV_h	Mean Magnitude μ_h Matching of EN 50160 Limits			Phase-Shift	$<THD_v>$ [%]			$<\Delta\theta_{tot}>$ [°C]
						Exact	+25%	−25%	
(a)	0.1	Exact	25%-above	25%-below	worst case	8.3	10.0	6.2	0
(b)	0.1	Exact	25%-above	25%-below	best case	8.3	10.0	6.2	0
(c)	0.1	Exact	25%-above	25%-below	experimental	8.3	10.0	6.2	0
(d)	0.3	Exact	25%-above	25%-below	worst case	6.5	8.1	4.8	0
(e)	0.3	Exact	25%-above	25%-below	best case	6.5	8.1	4.8	0
(f)	0.3	Exact	25%-above	25%-below	experimental	6.5	8.1	4.8	0
(g)	0.1	Exact	25%-above	25%-below	worst case	8.3	10.0	6.2	−15
(h)	0.1	Exact	25%-above	25%-below	best case	8.3	10.0	6.2	−15
(i)	0.1	Exact	25%-above	25%-below	experimental	8.3	10.0	6.2	−15
(j)	0.3	Exact	25%-above	25%-below	worst case	6.5	8.1	4.8	−15
(k)	0.3	Exact	25%-above	25%-below	best case	6.5	8.1	4.8	−15
(l)	0.3	Exact	25%-above	25%-below	experimental	6.5	8.1	4.8	−15

The reliability model for distorted current and voltage (36)–(39) is applied to these 36 case studies for estimating the life and reliability of:

- cross-linked polyethylene (XLPE)-insulated cables and all-film polypropylene (PP) insulated capacitors for MV/LV power systems, already examined in [8,9];
- induction motors and MV/LV transformers, tackled here for the first time in the streamline of this investigation.

The values of the parameters of Equations (36)–(39) used in the application are quoted in Table 2. As far as the cable and the capacitor are concerned, the values of n_p, n_w, n_r—derived by processing the results of ALTs performed on insulating samples subjected to various combinations of voltage harmonics [11,12]—and of B in Table 2 are the same as in [8,9] for the sake of comparison, but here the analysis is broader and different with respect to that carried out in [8,9]. Indeed here, as partly explained above:

- the case studies treated here are many more. In particular, the 24 cases with voltage harmonics 25% above and 25% below the limits in [4] are tackled for the first time, as outlined in Table 1;
- the chosen values of design life and probability are now set to 20 years and 1%, respectively, to be closer to the modern probabilistic design of power plant components on the one side, and to focus on the typical useful service life of the power plant;
- the chosen value of the shape parameter of Weibull distribution is 2 instead of 3 [8,9], in order to account for a milder degradation of component insulation during the life of the power plant.

Table 2. Values of the parameters of model (36)–(39) used in the application.

Component	β_t [adim.]	L_D [y]	P_D [%]	n_p [adim.]	n_w [adim.]	n_r [adim.]	B [K]
XLPE cable	2	20	1	14.80	4.90	1.20	12,430
All-film capacitor	2	20	1	6.20	0.56	1.80	12,500
induction motors	2	20	1	9.00	0.88	0.36	12,600
MV/LV transformers	2	20	1	11.00	0.99	0.44	12,600

As far as the induction motors and MV/LV transformers are concerned, the values of n_p, n_w, n_r and B in Table 2 have been derived by reprocessing the results in [10,51,52]. In fact, experimental results relevant to twisted pairs (i.e., twin varnished copper conductors wrapped on each other which reproduce on a smaller scale the full-size insulation of induction motors) indicate for n_p a value of 8–10, that can be used also for induction motor insulation. In the case of transformers, the dielectric performances of both epoxy resin and oil-paper insulation for MV/LV transformers suggest a slightly higher value, namely $n_p = 10 - 12$. For parameter B, a value of the order of those reported in Table 2 for the cable and the capacitor seems reasonable for both the induction motor and the transformer (from [52] a value of $B = 12{,}600$ can be derived for a bisphenolic epoxy resin), even if the thermal endurance of the epoxy insulation is usually larger than that of XLPE and PP.

A first observation drawn from Table 2 is that for all components the value of n_p overwhelms that of n_w and n_r; hence, K_p should have a foremost effect on the life and reliability of components subjected to voltage harmonics, if K_p, K_w and K_r have the same order of magnitude.

3.2. Results

For the XLPE cable and the all-film capacitor working in the distorted conditions of case studies (a)–(f) of Table 1, i.e., those relevant to $\Delta\theta_{tot} = 0$, as well as of case studies (g)–(l) of Table 1, i.e., those relevant to $\Delta\theta_{tot} = -15\,°C$, Table 3 reports the estimates of the following quantities:

- the 1st percentile of failure time, $t_{1\%,NS}$, in p.u. of design life L_D, computed via Equations (38) and (36);
- the reliability after a service time t_E equal to design life, $R(L_D)$, computed via Equations (39) and (37);

Table 3 also reports the 1st percentile of failure time, $t_{1\%,NS,OLD}$, in p.u. of design life L_D, computed via Equation (38) for $\Delta\theta_{tot} = 0$ with the voltage harmonics treated in [9] only, i.e., the 5th, 7th, 11th, 13th.

It is worth recalling that the cases 25% above and 25% below the limits after EN 50160 are totally new and treated here for the first time. Moreover, also the values of $t_{1\%,NS,OLD}$ in Table 3 differ from the values of the 1st percentile of failure time in [9]; indeed, the design hypothesis in [9] was to set the MTTF in sinusoidal conditions to 40 and 30 years for the cable and the capacitor, while here design life in sinusoidal conditions is set for both components to $L_D = 20$ years at design failure probability $P_D = 0.01 = 1\%$.

Analogously to Table 3, the homologous Table 4 reports for the induction motor and MV/LV transformer, working in the distorted conditions of case studies (a)–(f) ($\Delta\theta_{tot} = 0$) and (g)–(l) ($\Delta\theta_{tot} = -15\,°C$) of Table 1, the estimates of the following quantities:

- the 1st percentile of failure time, $t_{1\%,NS}$, in p.u. of design life L_D, computed via Equations (38) and (36);
- the reliability after a service time t_E equal to design life, $R(L_D)$, computed via Equations (39) and (37);

Table 4 also reports the 1st percentile of failure time, $t_{1\%,NS,OLD}$, in p.u. of design life L_D, computed via Equation (38) for $\Delta\theta_{tot} = 0$ with the voltage harmonics treated in [9] only, i.e., the 5th, 7th, 11th, 13th.

It is worth recalling that all cases in Table 4 are totally new and treated here for the first time, since they refer to the induction motor and the MV/LV transformer, tackled here for the first time in the streamline of this investigation.

Table 3. Values of 1st percentile of time to failure, $t_{1\%,NS}$, and reliability at rated life L_D, $R(L_D)$, estimated with reliability models (36)–(39) for the XLPE cable and the all-film capacitor subjected to 5th, 7th, 11th, 13th, 17th, 19th, 23rd, 25th voltage harmonics in case studies (a)–(f) ($\Delta\theta_{tot} = 0$), and (g)–(l) ($\Delta\theta_{tot} = -15\,^\circ$C), for the various matching of the limits in [4], see Table 1. The values of 1st percentile of time to failure, $t_{1\%,NS,OLD}$, calculated with the 5th, 7th, 11th, 13th voltage harmonics only as in [9], are also reported.

Component ↓	Estimated Quantity ↓	$\Delta\theta_{tot}$[°C]	Case Study → Limit Match ↓	(a)	(b)	(c)	(d)	(e)	(f)
cable	$t_{1\%,NS}$ [p.u. of L_D]	0	Strict	0.015	0.337	0.125	0.026	0.456	0.201
			25%-above	4.6×10^{-3}	0.213	0.052	7.9×10^{-3}	0.311	0.09
			25%-below	0.049	0.523	0.283	0.079	0.642	0.409
cable	$t_{1\%,NS,OLD}$ [p.u. of L_D]	0	Strict	0.054	0.510	0.203	0.087	0.628	0.200
			25%-above	0.023	0.368	0.103	0.039	0.487	0.101
			25%-below	0.124	0.681	0.378	0.183	0.775	0.381
cable	$R(L_D)$ [%]	0	Strict	3×10^{-18}	91.54	52.28	2.7×10^{-5}	95.28	77.90
			25%-above	$<10^{-18}$	80.08	2.526	$<10^{-18}$	90.10	29.21
			25%-below	1.505	96.39	88.24	20.21	97.59	94.18
capacitor	$t_{1\%,NS}$ [p.u. of L_D]	0	Strict	0.265	0.951	0.635	0.342	0.976	0.739
			25%-above	0.192	0.918	0.521	0.259	0.952	0.633
			25%-below	0.370	0.982	0.765	0.451	0.996	0.846
capacitor	$t_{1\%,NS,OLD}$ [p.u. of L_D]	0	Strict	0.380	0.959	0.658	0.461	0.978	0.654
			25%-above	0.297	0.930	0.555	0.376	0.958	0.550
			25%-below	0.486	0.983	0.771	0.564	0.993	0.773
capacitor	$R(L_D)$ [%]	0	Strict	86.69	98.90	97.54	91.75	98.95	98.17
			25%-above	76.05	98.82	96.36	86.07	98.90	97.52
			25%-below	92.92	98.96	98.30	95.19	98.99	98.61

Component↓	Estimated Quantity↓	ΔT_{tot}[°C]	Case study→Limit match↓	(g)	(h)	(i)	(j)	(k)	(l)
cable	$t_{1\%,NS}$ [p.u. of L_D]	−15	Strict	**0.065**	1.476	**0.545**	**0.113**	1.995	**0.876**
			25%-above	**0.020**	**0.931**	**0.229**	**0.035**	1.359	**0.395**
			25%-below	**0.214**	2.287	1.240	**0.347**	2.809	1.792
cable	$R(L_D)$ [%]	−15	Strict	**9.54**	99.54	**96.67**	45.35	99.75	**98.70**
			25%-above	**1.1×10^{-9}**	**98.85**	82.52	**2.5×10^{-2}**	99.46	**93.77**
			25%-below	**80.32**	99.81	99.35	**91.99**	99.87	99.69
capacitor	$t_{1\%,NS}$ [p.u. of L_D]	−15	Strict	1.170	4.196	2.801	1.508	4.305	3.259
			25%-above	**0.838**	4.018	2.280	1.133	4.165	2.771
			25%-below	1.619	4.297	3.346	1.975	4.360	3.703
capacitor	$R(L_D)$ [%]	−15	Strict	99.27	99.943	99.87	99.56	99.946	99.90
			25%-above	**98.58**	99.938	99.81	99.22	99.942	99.87
			25%-below	99.62	99.946	99.91	99.74	99.947	99.93

Table 4. Values of 1st percentile of time to failure, $t_{1\%,NS}$, and reliability at rated life L_D, $R(L_D)$, estimated with reliability models (36)–(39) for the induction motor and MV/LV transformer subjected to 5th, 7th, 11th, 13th, 17th, 19th, 23rd, 25th voltage harmonics in case studies (a)–(f) ($\Delta\theta_{tot} = 0$), and (g)–(l) ($\Delta\theta_{tot} = -15\,^\circ$C), for the various matching of the limits in [4], see Table 1. The values of 1st percentile of time to failure, $t_{1\%,NS,OLD}$, calculated with the 5th, 7th, 11th, 13th voltage harmonics only as in [9], are also reported.

Component ↓	Estimated Quantity ↓	$\Delta\theta_{tot}$ [°C]	Case Study → Limit Match ↓	(a)	(b)	(c)	(d)	(e)	(f)
motor	$t_{1\%,NS}$ [p.u. of L_D]	0	Strict	0.143	0.920	0.511	0.202	0.957	0.633
			25%-above	0.089	0.872	0.382	0.133	0.921	0.502
			25%-below	0.234	0.967	0.672	0.308	0.990	0.778
motor	$t_{1\%,NS,OLD}$ [p.u. of L_D]	0	Strict	0.244	0.937	0.542	0.319	0.965	0.537
			25%-above	0.170	0.896	0.422	0.235	0.936	0.417
			25%-below	0.349	0.973	0.684	0.430	0.988	0.686

Table 4. *Cont.*

Component ↓	Estimated Quantity ↓	$\Delta\theta_{tot}$ [°C]	Case Study → Limit Match ↓	(a)	(b)	(c)	(d)	(e)	(f)
motor	$R(L_D)$ [%]	0	Strict	61.31	98.82	96.22	78.22	98.91	97.52
			25%-above	28.06	98.69	93.34	56.51	98.82	96.08
			25%-below	83.20	98.93	97.80	89.94	98.98	98.35
transformer	$t_{1\%,NS}$ [p.u. of L_D]	0	Strict	0.095	0.924	0.449	0.141	0.963	0.577
			25%-above	0.053	0.872	0.317	0.084	0.924	0.435
			25%-below	0.171	0.974	0.624	0.236	0.997	0.741
transformer	$t_{1\%,NS,OLD}$ [p.u. of L_D]	0	Strict	0.180	0.936	0.478	0.246	0.966	0.473
			25%-above	0.117	0.891	0.354	0.169	0.934	0.349
			25%-below	0.278	0.974	0.633	0.356	0.991	0.636
transformer	$R(L_D)$ [%]	0	Strict	32.67	98.83	95.14	60.17	98.92	97.03
			25%-above	2.886	98.69	90.49	23.80	98.83	94.83
			25%-below	70.96	98.95	97.45	83.47	98.99	98.19

Component↓	Estimated Quantity↓	ΔT_{tot}[°C]	Case study→Limit match↓	(g)	(h)	(i)	(j)	(k)	(l)
motor	$t_{1\%,NS}$ [p.u. of L_D]	−15	Strict	**0.639**	4.103	2.277	**0.902**	4.269	2.823
			25%-above	**0.397**	3.889	1.703	**0.592**	4.107	2.236
			25%-below	1.042	4.313	2.997	1.373	4.413	3.469
motor	$R(L_D)$ [%]	−15	Strict	**97.57**	99.940	99.81	**98.77**	99.945	99.87
			25%-above	**93.81**	99.934	99.65	**97.17**	99.940	99.80
			25%-below	99.08	99.946	99.89	99.47	99.948	99.92
transformer	$t_{1\%,NS}$ [p.u. of L_D]	−15	Strict	**0.423**	4.118	2.003	**0.627**	4.293	2.573
			25%-above	**0.237**	3.890	4.122	**0.373**	4.122	1.940
			25%-below	**0.763**	4.341	2.781	1.052	4.444	3.305
transformer	$R(L_D)$ [%]	−15	Strict	**94.53**	99.941	99.75	**97.48**	99.945	99.85
			25%-above	**83.67**	99.934	99.50	**93.03**	99.941	99.73
			25%-below	**98.29**	99.947	99.87	99.10	99.949	99.91

Figure 3 illustrates the reliability vs. service time (in p.u. of design life) for the XLPE cable with $\Delta\theta_{tot} = 0$ and voltage harmonics that: (a) exactly match, (b) are 25% above, (c) are 25% below the limits in [4]. In the legend, $R_S(t)$ indicates reliability vs. time in the rated sinusoidal case, while $R_a(t)$, $R_b(t)$, $R_c(t)$, $R_d(t)$, $R_e(t)$, $R_f(t)$, denotes reliability vs. time in distorted case studies (a)–(f).

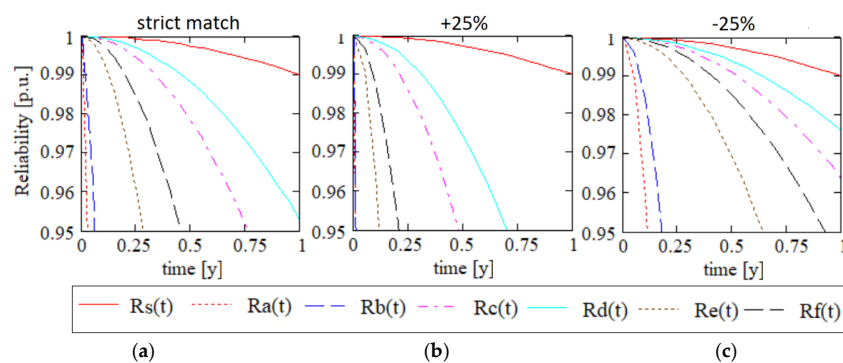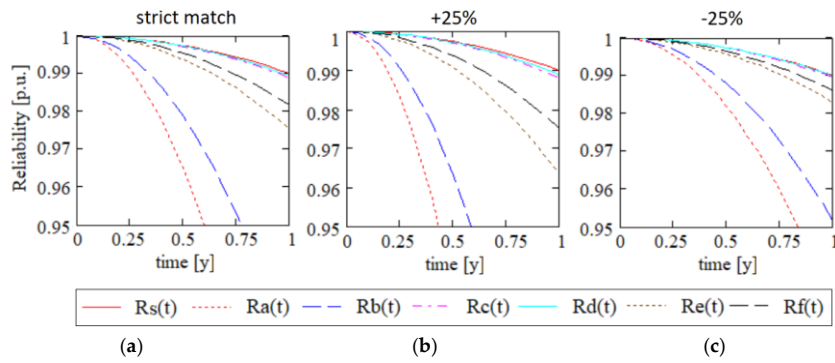**Figure 3.** Reliability vs. service time (in p.u. of design life) for the XLPE cable with voltage harmonics that: (**a**) exactly match, (**b**) are 25% above, (**c**) are 25% below the limits in [4]. $\Delta\theta_{tot} = 0$.

Figure 4 shows the same quantities in the same conditions as Figure 3, but for the capacitor. Similar figures could have been drawn for the induction motor and MV/LV transformer, but they are omitted here for brevity.
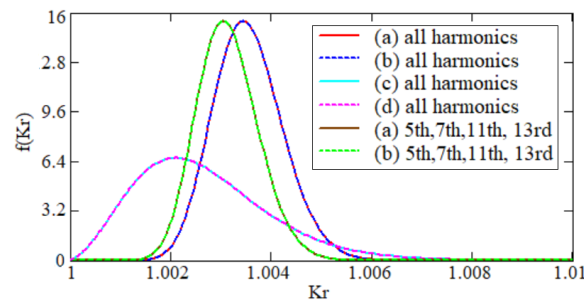
Figure 4. Reliability vs. service time (in p.u. of design life) for the all-film capacitor with voltage harmonics that: (**a**) exactly match, (**b**) are 25% above, (**c**) are 25% below the limits in [4]. $\Delta\theta_{tot} = 0$.

Figure 5a, reports the pdfs of K_p for case studies (a), (b), (c) with the strict match of the limits in [4] in the presence of the 5th, 7th, 11th, 13th, 17th, 19th, 23rd, 25th voltage harmonics, as well as of the 5th, 7th, 11th, 13th only as in [9]. Figure 5b is the same as Figure 5a, but for K_r instead of K_w. Figure 6 displays the pdfs of K_r for case studies (a), (b), (c), (d) with the 5th, 7th, 11th, 13th, 17th, 19th, 23rd, 25th voltage harmonics, as well as for case studies (a), (b) with 5th, 7th, 11th, 13th only.
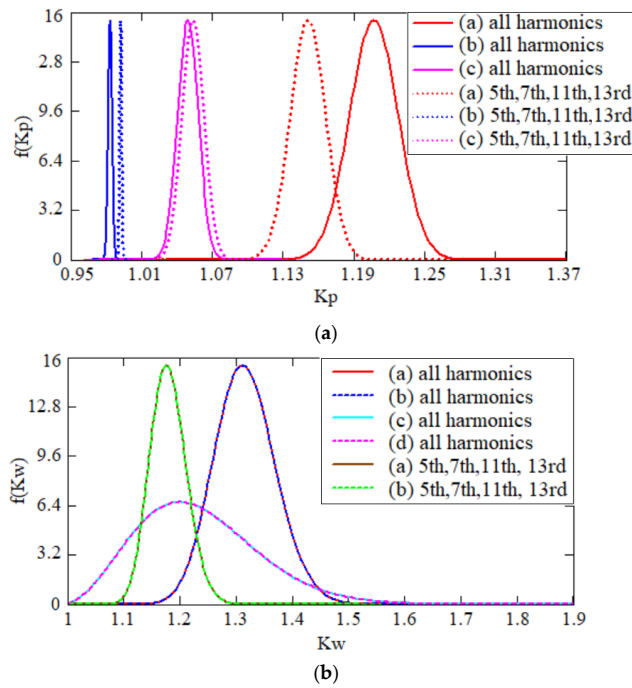

Figure 5. Probability density functions of: (**a**) K_p for case studies (a), (b), (c) with the strict match of the limits in [4] in the presence of the 5th, 7th, 11th, 13th, 17th, 19th, 23rd, 25th voltage harmonics, as well as of the 5th, 7th, 11th, 13th only; (**b**) K_w for case studies (a), (b), (c), (d) with the strict match of the limits in [4] in the presence of the 5th, 7th, 11th, 13th, 17th, 19th, 23rd, 25th voltage harmonics, as well as for case studies (a), (b) with 5th, 7th, 11th, 13th only.

Figure 6. Probability density functions of K_r for case studies (a), (b), (c), (d) with the strict match of the limits in [4] in the presence of the 5th, 7th, 11th, 13th, 17th, 19th, 23rd, 25th voltage harmonics, as well as for case studies (a), (b) in the presence of the 5th, 7th, 11th, 13th only.

Figure 7 illustrates the reliability vs. service time (in p.u. of design life) for the XLPE cable with $\Delta\theta_{tot} = -15\,°\text{C}$ and voltage harmonics that: (a) exactly match, (b) are 25% above, (c) are 25% below the limits in [4].
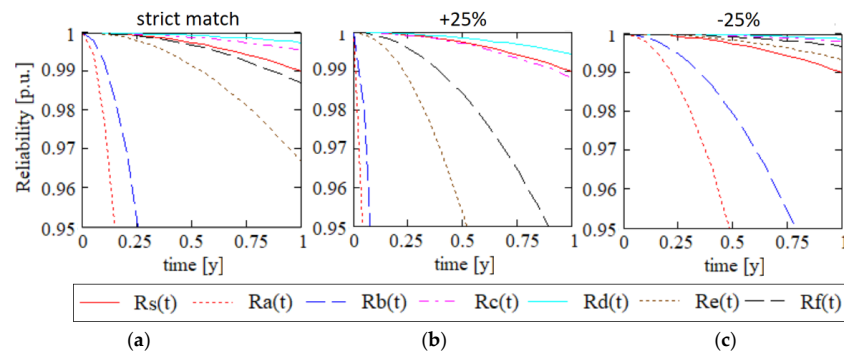
Figure 7. Reliability vs. service time (in p.u. of design life) for the XLPE cable with voltage harmonics that: (**a**) exactly match, (**b**) are 25% above, (**c**) are 25% below the limits in [4]. $\Delta\theta_{tot} = -15\,°\text{C}$.

3.3. Discussion

3.3.1. The Effect of Voltage Harmonics Only

Let us discuss the results of case studies (a)–(f) in Table 3 first, so as to deal with the effect of voltage harmonics only. The 1st percentile of failure time is lower—in most cases far lower—than design life for all case studies (a)–(f) and for both the cable and the capacitor; correspondingly, the reliability at design life L_D is always lower than design reliability $R_D = 1 - P_D = 0.99 = 99\%$. Hence, for such devices a combination of the 5th, 7th, 11th, 13th, 17th, 19th, 23rd, 25th voltage harmonics seems to be detrimental irrespective of their phase-shift angle.

This is also confirmed by the plots of reliability vs. service time for the cable and the capacitor reported in Figures 3 and 4, respectively, which show that the reliability in distorted cases (a)–(f) is always below that in rated sinusoidal conditions (solid red curve). Surprisingly, this holds not only when the harmonics comply with the limits in [4] exactly—as already found in [8] for the 11th, 13th harmonics and in [9] for the 5th, 7th, 11th, 13th—but also when they are 25% below these limits: hence, this analysis suggests that the distorted voltage waveshapes of case studies (a)–(f) can reduce the life and reliability of the insulation of the cable and the capacitor with respect to design life and reliability even if harmonics have a 25% safety margin compared to the limits in standards [2–4].

Obviously, the lowest values of $t_{1\%,NS}$ are found when harmonics are 25% above the limits: thus the limits in [4] are still a key reference for designing effective filters to limit voltage harmonics [31].

The effect on insulation life and reliability is different among cases (a)–(f): indeed, Table 3 and Figures 3 and 4 indicate that the reduction of component life and reliability is:

(1)   the greatest for worst cases (a), (d) leading to the highest peak of distorted voltage, see Figure 2a;

(2)   the smallest for best cases (b), (e) leading to the lowest peak of distorted voltage, see Figure 2b;

(3)   intermediate for experimental cases (c), (f) leading to an intermediate peak of distorted voltage, see Figure 2c.

From Table 3, case studies (a)–(f), it is also clear that the 1st percentile of failure time and reliability at design life increase as CV_h rises from 0.1 for cases (a), (b), (c) to 0.3 for cases (d), (e), (f)—i.e., with the scatter of the magnitude of voltage harmonics. This is because the 95th percentiles of the magnitude of voltage harmonics are fixed—i.e., either equal to, or 25% above, or 25% below the limits in [4]—and greater dispersion means that the cdfs $F(V_h)$/pdfs $f(V_h)$ encompass lower values of V_h, as deduced by comparing Figure 1b with Figure 1a.

Overall, it is worth emphasizing again that the calculations in this paper for the cable and the capacitor—summarized in Table 3—are completely new compared to those in previous ones [8,9], that have intentionally been cited here to allow a direct comparison. Such comparison shows that all results and figures in this paper—although being intentionally homologous to those in previous papers for enabling a straightforward comparison—are different as for the values obtained and the curves plotted from those reported in the previous papers. However, although being different, the results reported in this paper for the cable and the capacitor are in line with those previously obtained, but is also interesting to observe that—for both the cable and the capacitor—the whole sequence of odd voltage harmonics from the 5th to the 25th analysed here is more challenging than the simple combination of the 5th, 7th, 11th, 13th voltage harmonics treated in [9]. Indeed, in Table 3 the values of $t_{1\%,NS,}$ are all lower than the homologous values of $t_{1\%,NS,O}$: thus, it is worth performing the much more cumbersome analysis carried out here, since it is not only more accurate, but also on the safe side from the viewpoint of life and reliability estimation of power components.

Another essential comment stemming from the results in Table 3 and Figures 3 and 4 for case studies (a)–(f) is that the main outcomes hold for both the cable and the capacitor. Therefore, these outcomes seem to be general and independent of the values of n_p, n_w and n_r and of the uncertainty in their evaluation: indeed, in Table 2 the values of exponents n_p, n_w and n_r for the cable are far apart from those for the capacitor, thus their effect on a same set of values of K_p, K_w, K_r will be different as well.

This comment gives a chance of a deeper understanding of cases (a)–(f), which requires dealing precisely with the values of K_p, K_w, K_r. In fact, it should be understood that the values of K_p, K_w, K_r are not the same, either in a given case study, or among different case studies, as outlined in Figures 5 and 6.

Starting from Figure 5a, it is readily seen that the pdfs of K_p in case studies (a)–(c) fully agree with what previously observed at points (1)–(3) above for the same case studies, i.e., the pdf of K_p is located in correspondence of:

(i)   the highest values of K_p—always >1—for worst case (a). Thus, in this case study the peak value of distorted voltage fosters a strong reduction of life and reliability, as n_p>>1 (see Table 2);

(ii)   the smallest values of K_p—almost always slightly <1—for best case (b). Thus, in this case study the peak value of distorted voltage fosters a slight, but non-negligible increase of life;

(iii) intermediate values of K_p—almost always >1—for experimental case (c). Thus, in this case study the peak value of distorted voltage fosters a reduction of life, but less than in the worst case (a).

Furthermore, Figure 5a shows that the pdfs of cases (a), (b), (c) are located differently when the 5th, 7th, 11th, 13th voltage harmonics only are dealt with: the consideration of all harmonics moves the pdf of K_p towards higher values in case (a), slightly lower values in cases (b), (c). This agrees well with Figure 2a–c, since Figure 2a exhibits a higher peak of distorted voltage, while Figure 2b,c a slightly lower peak of distorted voltage when all harmonics are considered rather than the 5th, 7th, 11th, 13th only. This is due to the more favourable combination of phase-shift angles of cases (b),(c) when all harmonics than when the 5th, 7th, 11th, 13th only are included, since a better compensation of the peaks of the various harmonics is achieved in the former than in the latter case.

Analogous comments hold for the pdfs of K_p in the worst case (d), best case (e) and experimental case (f)—omitted in Figure 5a for brevity. However, in these case studies the pdfs of K_p are displaced towards lower values, for the same reasons explained above for the pdfs of V_h: namely cases (d), (e), (f) have a higher CV_h—0.3 vs. 0.1—than cases (a), (b), (c).

Anyway, as pointed out above when commenting on Table 3, the life and reliability of components is lower when all harmonics are considered. This is mainly because of the effect of the shape factor K_w, as straightforwardly understood from Figure 5b. Figure 5b—when compared to Figure 5a—demonstrates that, while K_p depends strongly on phase-shift angles ϕ_h, K_w does not, since it is affected only by the order h and rms value V_h of voltage harmonics, see Equations (7)–(9). Thus the pdf of K_w is the same for worst case (a) as for best case (b) and experimental case (c) (this latter omitted in Figure 5b for the sake of graphical clearness)—since these cases differ only as for the values of ϕ_h. Similarly, the pdf of K_w is the same for worst case (d) as for best case (e) and experimental case (f) (this latter omitted, too). However, when all voltage harmonics are considered the pdf of K_w moves towards much higher values than with the 5th, 7th, 11th, 13th harmonics only, and since exponent n_w is significantly >1—although being much lower than n_p—this involves that life and reliability of the component with all voltage harmonics decrease with respect to the 5th, 7th, 11th, 13th harmonics only. On the other hand, such a decrease is much more remarkable for the cable than for the capacitor, as n_w is much higher for the former than for the latter.

One could guess the rms factor K_r plays a more significant role than K_w for the capacitor. Indeed, as shown in Table 2, the capacitor features $n_r = 1.8 > n_w = 0.56$, while the cable features $n_r = 1.2 << n_w = 4.9$. This is not true, as seen in Figure 6—the same as Figure 5b, but for K_r instead of K_w. In fact, Figure 6 shows that $K_r \approx 1$ in all case studies treated here (Experimental cases (c) and (f) are omitted in Figure 6 like in Figure 5b for the sake of graphical clearness, since they yield the same pdfs as cases (a),(b) and (d),(e), respectively.), hence its effect on life and reliability of power components is negligible in these cases. This conclusion can be essentially generalized to the most applicable cases, unless the total harmonic distortion of voltage THD_V is really severe, say, above 20% (see Equation (10) for the relationship between THD_V and K_r): here $THD_V \leq 10\%$, see Table 1.

Figures 5 and 6 also confirm that—as stated in Section 2.1 when commenting on Equations (7)–(9)—K_p can be either <1 or >1, while K_w and K_r are always ≥1. However, K_w can attain much higher values than:

- K_p, as straightforwardly understood when comparing Figure 5b with Figure 5a;
- K_r in particular, as readily seen by comparing Figure 5b with Figure 6.

Like the pdf of K_p, also the pdfs of K_w and K_r are displaced towards lower values of K_w and K_r for a higher dispersion: the reason is same as for the pdfs of V_h and K_p, see above.

As for the differences between the cable and the capacitor, all quantities in Table 3 are much greater for the all-film capacitor than for the XLPE cable in all case studies. This is because the cable features much greater values of the exponents n_p and n_w (see Table 2), which weigh the role played by K_p and K_w, the most dominant ageing factors not only in the case studies analysed here, but under distorted voltage in general [35,36]. On the other hand, unforeseen parallel resonances between the capacitor and the equivalent impedance of the grid—skipped here for the sake of brevity—might increase a few voltage harmonics strongly, thereby causing a premature failure of the capacitor.

Another difference between capacitor and cable is that the former is truly placed at a certain node in the network, where voltage distortion changes only with time, while cable lines actually stretch from one node to another, experiencing a voltage distortion that typically changes both with time and along the line. Hence, voltage distortion at a given time is more or less deterministically distributed along cable lines. Here cables are implicitly regarded as a discrete number of series-connected cable lengths with a constant—in space—voltage distortion level within each length.

Coming now to the induction motor and the transformer, as done in the case of Table 3 for the cable and the capacitor, let us discuss the results of case studies (a)–(f) in Table 4 first, so as to deal with

the effect of voltage harmonics only. Table 4 confirms the following observations already made when commenting on the homologous case studies (a)–(f) in Table 3 for the cable and the capacitor.

(1) The 1st percentile of failure time is lower—in most cases far lower—than design life for all case studies (a)–(f) and for both the induction motor and the transformer; correspondingly, the reliability at design life L_D is always lower than design reliability $R_D = 1-P_D = 0.99 = 99\%$. Hence, for such devices a combination of the 5th, 7th, 11th, 13th, 17th, 19th, 23rd, 25th voltage harmonics seems to be detrimental irrespective of their phase-shift angle.

(2) Surprisingly, this holds not only when the harmonics comply with the limits in [4] exactly, but also when they are 25% below these limits. Hence, this analysis suggests that the distorted voltage waveshapes of case studies (a)–(f) can reduce the life and reliability of the insulation of the induction motor and the transformer with respect to design life and reliability even if harmonics have a 25% safety margin compared to the limits in standards [2–4].

(3) Obviously, the lowest values of $t_{1\%,NS}$ are found when harmonics are 25% above the limits. Thus also for the induction motor and the transformer the limits in [4] are a key reference for designing effective filters to limit voltage harmonics.

(4) The effect on insulation life and reliability is different among cases (a)–(f). Indeed, Table 4 indicates that the reduction of component life and reliability is:

    (i) the greatest for worst cases (a), (d) leading to the highest peak of distorted voltage, see Figure 2a;

    (ii) the smallest for best cases (b), (e) leading to the lowest peak of distorted voltage, see Figure 2b;

    (iii) intermediate for experimental cases (c), (f) leading to an intermediate peak of distorted voltage, see Figure 2c.

(5) The 1st percentile of failure time and reliability at design life increase as CV_h rises from 0.1 for cases (a), (b), (c) to 0.3 for cases (d), (e), (f)—i.e., with the scatter of the magnitude of voltage harmonics.

(6) For both the induction motor and the transformer the whole sequence of odd voltage harmonics from the 5th to the 25th analysed here is more challenging than the simple combination of the 5th, 7th, 11th, 13th voltage harmonics treated in [9]. Indeed, in Table 4 the values of $t_{1\%,NS,}$ are all lower than the homologous values of $t_{1\%,NS,O}$: thus, it is worth performing the much more cumbersome analysis carried out here, since it is not only more accurate, but also on the safe side from the viewpoint of life and the reliability estimation of power components subjected to harmonics generated by power electronic converters (cables, capacitors, induction motors, transformers).

(7) The main outcomes hold for both the induction motor and the transformer, as well as for the cable and the capacitor before, thus for all treated components. Therefore, these outcomes seem to be general and independent of the values of n_p, n_w and n_r and of the uncertainty in their evaluation. Indeed, in Table 2 the values of exponents n_p, n_w and n_r differ more or less remarkably among the various components, thus their effect on a same set of values of K_p, K_w, K_r will be different as well.

Other comments stemming from a comparison between Table 3 for the cable and the capacitor and Table 4 for the transformer and induction motor—as well as from the inspection of Figure 5—is that the role played by K_w vs. K_p is more noteworthy for the cable, less significant for the other components, essentially because the capacitor, motor and transformer have all a lower value of n_w, as readily seen in Table 2. In this respect it can be said that the motor and transformer have a closer behavior to the capacitor than to the cable; this is not surprising, when considering that typically the composite/lapped structure of the insulation of motors and MV/LV transformers is more similar to the lapped insulation of the PP capacitor than to the quasi-homogeneous insulation of the XLPE cable.

On the other hand, it is also interesting to point out that the motor and the transformer exhibit lower values of time to failure and reliability than the capacitor in the same case studies. This is essentially due to the higher value of n_p featured by the motor ($n_p = 9$) and the transformer ($n_p = 11$)

compared to the capacitor (n_p = 6.2). For the same reason, in turn, the transformer exhibits lower values of time to failure and reliability than the motor in the same case studies.

In summary, the hierarchy of the values of failure times and reliability is as follows: capacitor < motor < transformer < cable. However, it should be pointed out that this hierarchy has to be taken with great care, since it has been obtained from the values of reliability model parameters reported in Table 2, which are subjected to all uncertainties related to the relevant experimental campaigns and failure of data processing. Moreover, these values hold for the particular insulating specimens considered in those campaigns, which of course cannot be considered as fully representative of all insulations of existing capacitors, motors, transformers and cables found in MV and LV systems.

3.3.2. The Effect of Current Harmonics and Sinusoidal Current

Coming now to the effect of current harmonics, one could guess that the relevant Joule losses might cause a further reduction of lifetime and reliability of power components compared to those quoted for case studies (a)–(f) in Table 3 and in Table 4, as outlined in [6,7]. However, load demand and common service practices imply that distribution grids and the relevant power components mostly work at a load substantially lower than the design "sinusoidal" load. In this way, the thermal effect of harmonic currents is insufficient to let the maximum temperature of components reach the rated sinusoidal temperature. This is also because some design practices recommended to oversize conductors to be on the safe side as for possible harmonic currents. This situation, rather common especially for MV distribution cables [50], might hide the decrease of life and reliability under distorted voltage found for case studies (a)–(f) in Table 3. To check this effect, Table 3 includes case studies (g)–(l), identical to case studies (a)–(f) apart that $<\Delta\theta_{tot}> = <\Delta\theta_{arm}> + <\Delta\theta_{HL}> = -15$ °C (see Table 1).

Case studies (g)–(l) in Tables 3 and 4 show that this effect can really occur. Indeed, for the treated components all values of failure times and reliability increase significantly in case studies (g)–(l) with respect to their homologous values in case studies (a)–(f). In particular, the 1st percentile of time to failure rises by a factor $exp(-B\langle\Delta T'_{tot}\rangle)$—compare Equation (36) with Equation (38)—which is ≈4.4 for the cable and the capacitor, ≈4.5 for the motor and the transformer: thus this factor is quite similar for all treated components, since the relevant values of B are quite close (see Table 2). However, being times to failure at $<\Delta\theta_{tot}> = 0$ °C the highest for the capacitor, the least for the cable, intermediate for the motor and the transformer, the increase involved by $<\Delta\theta_{tot}> = -15$ °C leads to:

- values of the 1st percentile of time to failure more or less broadly above design life (thus values of reliability at design life more or less broadly >99%) in all case studies for the capacitor—apart case (a) with voltage harmonics 25% above the limits in [4] (see bold numbers in Table 3);
- values of the 1st percentile of time to failure below design life (thus values of reliability at design life <99%) in worst cases (g) and (j) with voltage harmonics matching exactly or 25% above the limits in [4] for the motor (see bold numbers in Table 4);
- values of the 1st percentile of time to failure below design life (thus values of reliability at design life <99%) in the following case studies for the transformer (see bold numbers in Table 4):

  - worst case (g) with all matching types of the limits in [4];
  - worst case (j) with voltage harmonics matching exactly or 25% above the limits in [4];

- values of the 1st percentile of time to failure below design life (thus values of reliability at design life <99%) in the following case studies for the cable (see bold numbers in Table 3):

  - worst cases (g) and (j) with all matching types of the limits in [4];
  - experimental cases (i) and (l) with voltage harmonics matching exactly or 25% above the limits in [4];

- values of the 1st percentile of time to failure more or less broadly above design life (thus reliability at design life more or less broadly >99%) in best cases (h) and (k) for the cable.

Focusing on the cable, these potentially harmful cases are also confirmed by the plots of reliability vs. service time for the cable with $<\Delta\theta_{tot}> = -15\ °C$ reported in Figure 7, which show the many previously listed cases where cable reliability in distorted conditions falls below that in rated sinusoidal conditions (solid red curve). Therefore, as such "pessimistic" cases cannot be fully ruled out for a cable subjected to voltage and current harmonics generated by power electronic devices, such a cable faces a risk of premature failure although its average temperature is 15 °C below design temperature. This holds also for potentially harmful cases for the motor and the transformer emphasized with bold characters in Table 4.

3.3.3. Further Remarks

As a closure of this discussion, it must be emphasized that the analysis carried out here in the streamline of the present investigation does not have a particular type of converter as a reference—e.g., the 6-pulse or the 12-pulse, although the 6-pulse and 12-pulse SCR-based converters are quite often encountered in LV and MV grids. Rather, this analysis aims at reproducing the typical situation of harmonic distortion level which can be typically found in LV and MV grids, based on the typical distorting loads found in such grids and on the typical filtering strategies to limit the effects of such distorting loads. This is the reason why international standards EN50160, IEC 61000-2-2, IEC 61000-2-4 are taken as a reference here; based on the limitations established by these authoritative international standards to voltage harmonics—and in particular by the probabilistically-established limits after EN50160—we have chosen as case-study examples three typical sets of possible voltage distortion levels, i.e.,:

- exact match of the limits, in order to reproduce situations where the plant is designed so as to comply with the limits, but with no safety margins (to spare money);
- 25% below the limits, in order to reproduce situations where the plant is designed so as to comply with the limits with a heuristically found and apparently broad enough safety margin, thereby spending more money than strictly needed to increase the power quality of the grid;
- 25% above the limits, in order to reproduce situations where the plant is designed carelessly with respect to the limits (this might happen from time to time in huge industrial plants with their own MV and LV grids to spare further money).

However, each of these three criteria is only one among infinite possible ways to set the voltage distortion level. Once the distortion level is set parametrically or known from measurements in a particular point of common coupling (PCC) in the grid or internal point of coupling (IPC) in a plant, the method proposed here—namely Equations (31)–(39)—can be applied anyway.

4. Conclusions

This paper has refined the theory and broadened the applications of an electro-thermal probabilistic life model—also referred to as electro-thermal reliability model—developed in previous studies for the insulation of power components affected by current and voltage harmonics. In line with previous papers, the outcomes of this article confirm that the limits to voltage harmonics set in international standards may be not totally conservative as for the reliability of components subjected to the harmonics generated by power electronic converters. This holds even if a fairly broad safety margin of 25% is kept from such limits. This effect is due not only to the peak of the distorted voltage, accounted for by the peak factor K_p, but also to the shape of the distorted voltage—thus to its time derivative—accounted for by the shape factor K_w. The effect of voltage harmonics may be compensated for by a lower-than-rated load current of components. However, only a strong reduction of the load can hide the effect of distorted voltage totally.

Another important conclusion of this study is that for all treated components (cables, capacitors, induction motors, transformers) and for all case studies examined, the whole sequence of odd voltage harmonics from the 5th to the 25th analysed here is more challenging that the simple combination of

the 5th, 7th, 11th, 13th voltage harmonics treated previously. Thus, it is worth performing the much more cumbersome analysis carried out here, since it is not only more accurate, but also on the safe side from the viewpoint of life and reliability estimation of power components.

The results also point out that a wide variety of distorted regimes can be encountered in practice, each having different effects on component reliability. Therefore, a reliability model like that presented here is a quite useful tool to be used in each case of interest beside other methods, like careful experimental measurements and sound diagnostic techniques. All these techniques employed together may provide a fairly exhaustive picture of the effect of voltage and current harmonics generated by power electronic devices on the life and reliability of power components.

It is also worth emphasizing that the reliability model is used here for life and reliability estimates of the MV/LV capacitor and cable, but it can be extended to other insulations, e.g., those of induction motors and transformers. Indeed, the treated components feature quite different values of the parameters of the reliability model: since the main results obtained here for all case studies hold for both the cable and the capacitor, these results appear to be general and independent of the values of the parameters, as well as of the uncertainty in their evaluation.

Furthermore, the investigations presented in this paper for the international standards EN50160, IEC 61000-2-2, and IEC 61000-2-4 could be conducted in future works considering also other standards from the IEC 61000 series that are related to specific equipment and converters.

As a final remark, it has to be pointed out that—due to the simplifying assumptions made and the "quasi-parametric" approach followed—the results obtained should be always generalized with care, being indicative but not exhaustive. Indeed, all results reported here have been obtained from particular values of reliability model parameters, which are subjected to all uncertainties related to the relevant experimental campaigns and failure of data processing. Moreover, these values hold for the particular insulating specimens considered in those campaigns, which of course cannot be considered as fully representative of all insulations of existing capacitors, motors, transformers and cables found in MV an LV system.

References

1. IEEE Standard 519-1992. *IEEE Recommended Practices and Requirements for Harmonic Control. in Electric Power Systems*; IEEE: Piscataway, NJ, USA, 1993.
2. IEC Standard 61000-2-2. *Environment—Compatibility Levels for Low-Frequency Conducted Disturbances and Signalling in Public Low-Voltage Power Supply Systems*; IEC: Geneva, Switzerland, 2002.
3. IEC Standard 61000-2-4. *Environment—Compatibility Levels in Industrial Plants for Low-Frequency Conducted Disturbances*; IEC: Geneva, Switzerland, 2002.
4. European Standard EN Standard 50160. *Voltage Characteristics of Electricity Supplied by Public Distribution Networks*, 3rd ed.; European Committee for Standardization: Brussels, Belgium, 2010.
5. Chiodo, E.; Mazzanti, G. Theoretical and practical aids for the proper selection of reliability models for power system components. *Int. J. Reliab. Saf.* **2008**, *2*, 99–128. [CrossRef]
6. Mazzanti, G.; Passarelli, G. A probabilistic life model for reliability analysis of power cables feeding electric traction systems. In Proceedings of the 2006 IEEE International Symposium on Power Electronics, Electrical Drives, Automation and Motion IEEE SPEEDAM 2006, Taormina, Italy, 23–26 May 2006; pp. S30_17–S30_22.
7. Mazzanti, G.; Passarelli, G.; Russo, A.; Verde, P. The effects of voltage waveform factors on cable life estimation using measured distorted voltages. In Proceedings of the 2006 IEEE Power Engineering Society General Meeting IEEE PES GM 2006, Montreal, QC, Canada, 18–22 June 2006.

8. Mazzanti, G. Are the Limits to Harmonic Voltages given by International Standards on the Safe Side from the Viewpoint of Power Component Reliability? *Int. Rev. Electr. Eng. (IREE)* **2011**, *6*, 2762–2772.

9. Mazzanti, G. Reliability Evaluation of Insulation subjected to Harmonic Voltages within the Limits set by International Standards. *IEEE Trans. Dielectr. Electr Insul.* **2014**, *21*, 2037–2046. [CrossRef]

10. Cavallini, A.; Fabiani, D.; Mazzanti, G.; Montanari, G.C.; Contin, A. Voltage endurance of electrical components supplied by distorted voltage waveforms. In Proceedings of the International Symposium on Electrical Insulation (IEEE/ISEI), Anaheim, CA, USA, 2–5 April 2000; pp. 73–76.

11. Cavallini, A.; Fabiani, D.; Mazzanti, G.; Montanari, G.C. Models for degradation of self-healing capacitors operating under voltage distortion and temperature. In Proceedings of the 6th International Conference on Properties and Applications of Dielectric Materials (Cat. No.00CH36347), Xi'an, China, 6 August 2002; pp. 108–111.

12. Cavallini, A.; Mazzanti, G.; Montanari, G.C.; Fabiani, D. The effect of power system harmonics on cable endurance and reliability. In Proceedings of the IEEE IAS 35th Annual Meeting, Rome, Italy, 8–12 October 2000; pp. 240–247.

13. Montanari, G.C.; Fabiani, D. The effect of voltage distortion on ageing acceleration of insulation systems under partial discharge activity. *IEEE Ind. Electron. Mag.* **2001**, *17*, 24–33.

14. Sletbak, J.; Botne, A. A Study on Inception and Growth of Water Trees and Electrochemical Trees in Polyehtylene and Cross Linked Polyehtylene Insulations. *IEEE Trans. Electron. Insul.* **1977**, *12*, 383–389. [CrossRef]

15. Ildstad, E. *High. Voltage AC and DC Aging of an XLPE Distribution Cable in Wet Enviroment*; Nord-IS: Trondheim, Norway, 1988.

16. Ildstad, E.; Bardsen, H.; Faremo, H.; Knutsen, B. Influence of Mechanical and Frequency on Water Treeing in XLPE Cable Insulation. In Proceedings of the IEEE International Symposium on Electrical Insulation, Toronto, ON, Canada, 3–6 June 1990.

17. Ross, R. Inception and propagation mechanisms of water treeing. *IEEE Trans. Dielectr. Electr. Insul.* **1998**, *5*, 660–680. [CrossRef]

18. Mauseth, F.; Amundsen, M.; Lind, A.; Faremo, H. Water Tree Growth of Wet XLPE Insulation Stressed with DC and High Frequency AC. In Proceedings of the 2012 Annual Report Conference on Electrical Insulation and Dielectric Phenomena, Montreal, QC, Canada, 14–17 October 2012; pp. 692–695.

19. Patil, K.D.; Gandhare, W.Z. Threat of harmonics to underground cables. In Proceedings of the 2012 Students Conference on Engineering and Systems, Allahabad, Uttar Pradesh, 16–18 March 2012.

20. Sadati, S.B.; Yazdani-Asrami, M.; Taghipour, M. Effects of harmonic current content and ambient temperature on load ability and life time of distribution transformers. *Int. Rev. Electr. Eng.* **2010**, *3*, 1444–1451.

21. Bihari, S.; Goswami, U.; Goswami, A.; Sadhu, P.K. Fast Estimating Method of Effective Life of Power Cable in Industrial Environment. In Proceedings of the 2019 23rd International Conference Electronics, Palanga, Lithuania, 17–19 June 2019.

22. Yaghoobi, J.; Alduraibi, A.; Martin, D.; Zare, F.; Eghbal, D.; Memisevic, R. Impact of high-frequency harmonics (0–9 kHz) generated by grid-connected inverters on distribution transformers. *Int. J. Electr. Power Energy Syst.* **2020**, *122*, 106177. [CrossRef]

23. Thango, B.A.; Jordaan, J.A.; Nnachi, A.F. Effects of Current Harmonics on Maximum Loading Capability for Solar Power Plant Transformers. In Proceedings of the 2020 International SAUPEC/RobMech/PRASA Conference, Cape Town, South Africa, 29–31 January 2020.

24. Montanari, G.C. *Power Electronics and Electrical Apparatus: A Threat?* NORD-IS: Lingby, Denmark, 2007.

25. Cavallini, A.; Fabiani, D.; Montanari, G.C. Power electronics and electrical insulation systems—part 2: Life modeling for insulation design. *IEEE Electr. Insul. Mag.* **2010**, *26*, 33–39. [CrossRef]

26. Lebey, T.; Castelan, P.; Montanari, G.C.; Ghinello, I. Influence of PWM-type voltage waveforms on reliability of machine insulation system. In Proceedings of the 8th International Conference on Harmonics and Quality of Power. Proceedings, Athens, Greece, 14–16 October 1998.

27. Montanari, G.C.; Hebner, R.; Morshuis, P.; Seri, P. An Approach to Insulation Condition Monitoring and Life Assessment in Emerging Electrical Environments. *IEEE Trans. Power Deliv.* **2019**, *34*, 1357–1364. [CrossRef]

28. Carboni, A.; ElShawarby, K.; Foglia, G.M.; Perini, R.; Gerlando, A.D.; Ragaini, E. Electric Stress in Power Electronics Applications. In Proceedings of the 2019 IEEE Milan PowerTech, Milan, Italy, 23–27 June 2019.

29. Lv, C.; Liu, J.; Zhang, Y.; Lei, W.; Cao, R.; Lv, G. Reliability Modeling for Metallized Film Capacitors Based on Time-Varying Stress Mission Profile and Aging of ESR. *IEEE J. Emerg. Sel. Top. Power Electron.* **2020**. [CrossRef]

30. Borthakur, D.P.; Das, S. Life Estimation of XLPE Cable Under Electrical and Thermal Stress. In Proceedings of the International Conference on High Voltage Engineering and Technology (ICHVET), Hyderabad, India; 7–8 February 2019. [CrossRef]

31. Arillaga, J.; Bradley, D.A.; Bodge, P.S. *Power System Harmonics*; Wiley: New York, NY, USA, 1988.

32. Lamedica, R.; Marzinotto, M.; Prudenzi, A. Harmonic amplitude and harmonic phase angle monitored in an electrified subway system during rush hours traffic. In Proceedings of the 4th IASTED, Rhodes, Greece, 28–30 June 2004.

33. Caramia, P.; Carpinelli, G.; Verde, P.; Vitali, F. Probabilistic Evaluation of the Cable Thermal Useful Life in MV/LV Energy Systems. In Proceedings of the 5' International Conference on Probabilistic Methods applied to Power Systems, Vancouver, BC, Canada, 21–25 September 1997.

34. Caramia, P.; Carpinelli, G.; Russo, A.; Verde, P. Estimation of Thermal Useful Life of MV/LV Cables in Presence of Harmonics and Moisture Migration. In Proceedings of the IEEE Bologna Power Tech Conference, Bologna, Italy, 23–26 June 2003.

35. Gallo, D.; Langella, R.; Testa, A. Predicting voltage stress effects on MV/LV components. In Proceedings of the IEEE Bologna Power Tech Conference, Bologna, Italy, 23–26 June 2003.

36. Gallo, D.; Langella, R.; Testa, A. Is it always possible to separately analyze different power quality phenomena? The case of the voltage peak. *L'Energia Elettr.* **2004**, *81*, 162–167.

37. Montanari, G.C.; Mazzanti, G. From Thermodynamic to Phenomenological Multistress Models for Insulating Materials without or with evidence of Threshold. *J. Phys. D Appl. Phys.* **1994**, *27*, 1691–1702. [CrossRef]

38. Montanari, G.C.; Mazzanti, G.; Simoni, L. Progress in electrothermal life modeling of electrical insulation over the last decades. *IEEE Trans. Dielectr. Electr. Insul.* **2002**, *9*, 730–745. [CrossRef]

39. Mazzanti, G.; Montanari, G.C.; Simoni, L. Insulation Characterization in Multistress Conditions by Accelerated Life Tests: An Application to XLPE and EPR for High-Voltage Cables. *IEEE Electr. Insul. Mag.* **1997**, *13*, 24–33. [CrossRef]

40. Dissado, L.A.; Fothergill, J.C. *Electrical Degradation and Breakdown in Polymers*; Peregrinus: London, UK, 1992.

41. Mazzanti, G.; Marzinotto, M. *Extruded Cables for High. Voltage Direct Current Transmission: Advances in Research and Development*; Wiley-IEEE Press: Hoboken, NJ, USA, 2013.

42. Cacciari, M.; Mazzanti, G.; Montanari, G.C. Comparison of Maximum Likelihood Unbiasing Methods for the Estimation of the Weibull Parameters. *IEEE Trans. Dielectr. Electr. Insul.* **1996**, *3*, 18–27. [CrossRef]

43. Miner, M.A. Cumulative damage in fatigue. *J. Appl. Mech.* **1945**, A159–A163.

44. Ministerial Decree 6 July 2012—Incentives for Energy from Non-Photovoltaic Renewable Electricity Sources. Available online: https://www.mise.gov.it/index.php/it/normativa/decreti-ministeriali/2023799-decreto-ministeriale-6-luglio-2012-ed-allegati-incentivi-per-energia-da-fonti-rinnovabili-elettriche-non-fotovoltaiche (accessed on 13 May 2020).

45. Ministerial Decree 4 July 2019—Methods for Calculating Storage Obligations. Available online: https://www.gse.it/documenti_site/Documenti%20GSE/Servizi%20per%20te/FER%20ELETTRICHE/NORMATIVE/DM%204%20luglio%202019%20-%20Incentivazione%20dell%e2%80%99energia%20elettrica%20prodotta%20dagli%20impianti.pdf (accessed on 13 May 2020).

46. The National Renewable Energy Laboratory of the U.S. Department of Energy. Available online: https://www.nrel.gov/analysis/tech-footprint.html (accessed on 13 May 2020).

47. Chiodo, E.; Mazzanti, G. Mathematical and physical properties of reliability models in view of their application to modern power system components. In *Innovations in Power Systems Reliability*; Anders, G.J., Vaccaro, A., Eds.; Springer: London, UK, 2011; pp. 59–140.

48. Chiodo, E.; Mazzanti, G. Bayesian inference of power system insulation reliability in the presence of voltage harmonics. *Int. Rev. Electr. Eng.* **2016**, *11*, 266–276. [CrossRef]

49. Wang, Y.J.; Pierrat, L.; Wang, L. Summation of Harmonic Currents produced by AC/DC Static Converters with Randomly Fluctuating Loads. *IEEE Trans. Power Deliv.* **1994**, *9*, 1129–1135. [CrossRef]

50. Katz, C.; Seman, G.W.; Bernstein, B.S. Low temperature aging of XLPE and EP insulated cables with voltage transients. *IEEE Trans. Power Deliv.* **1995**, *10*, 34–42. [CrossRef]

51. Caramia, P.; Carpinelli, G.; Verde, P.; Mazzanti, G.; Cavallini, A.; Montanari, G.C. An approach to life estimation of electrical plant components in the presence of harmonic distortion. In Proceedings of the 9th IEEE International Conference on Harmonics and Quality of Power (IEEE ICHQP), Orlando, FL, USA, 1–4 October 2000.

52. Montanari, G.C.; Pattini, G. Thermal endurance of insulating materials. *IEEE Trans. Electr. Insul.* **1986**, *21*, 66–75.